Active Sensing

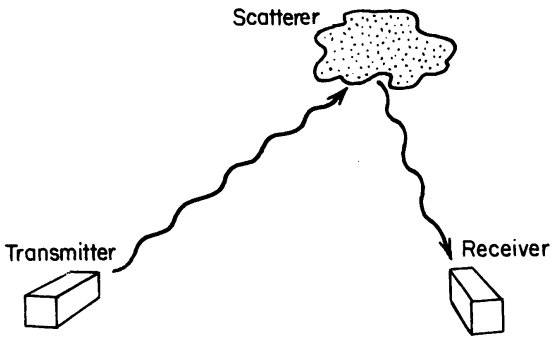

- Range resolved (pulsed) systems
- Frequency modulated systems

- Radar
  - radar equation
  - reflectivity properties
  - attenuation
  - dual polarization
- Lidar
  - Lidar equation
  - The lidar inversion problem: backscatter-to-extinction ambiguity
  - High spectral resolution lidar
  - lidar in space – multiple scattering
  - DIAL
- Doppler systems
  - Principles of Doppler wind measurement

- Strength of backscatter
- Polarization of backscatter
- Attenuation of pulse
- Phase change

For more information on Radar:

AT741 : Radar Meteorology

Topics Covered:

- Microwave scattering theory
- Radar engineering
- Doppler principles
- Polarimetric radar
- Dual-wavelength radar
- mm-wave radars

Radar & Lidar Wavelengths

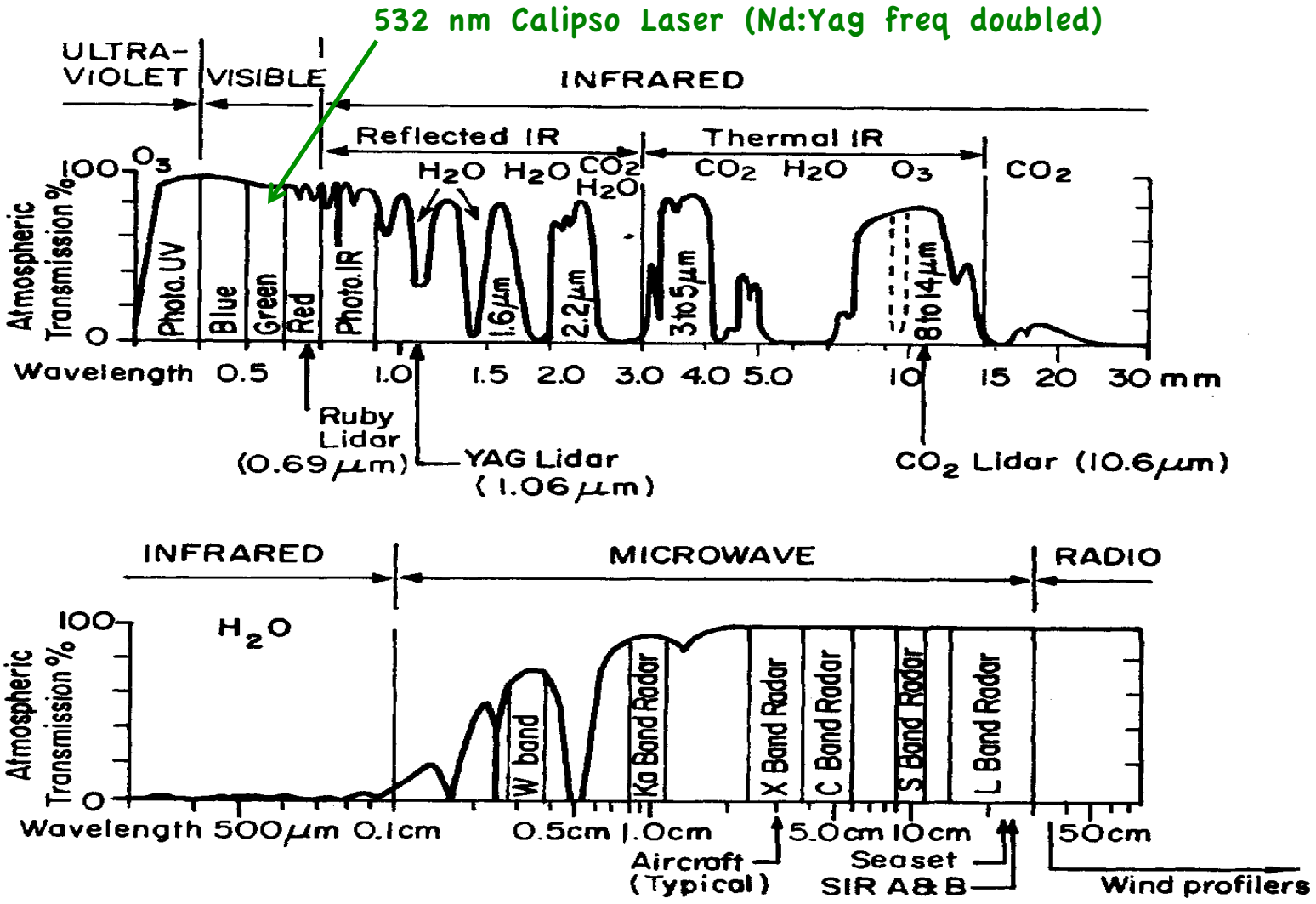

Characteristics of different transmitters

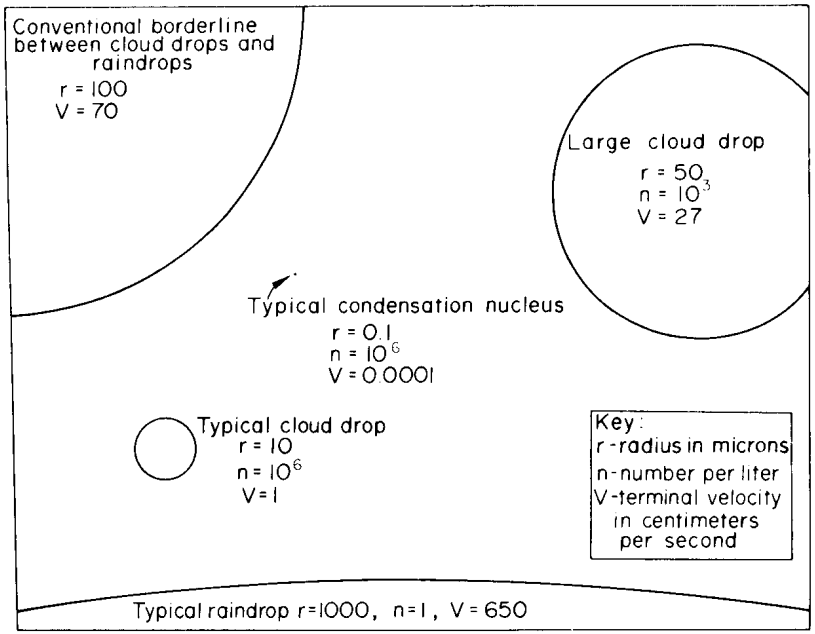

Transmitter	Advantage	Disadvantage
Laser (visible, infrared wavelengths; 0.5-10 X 10^{-6} m)	Sees* all particles of a few 0.1 X 10^{-6} m and greater, able to provide high resolution	Attenuates heavily in moderately thick cloud, multiple scattering confuses ranging (from space)
Mirowave		
mm wavelength (e.g. 3mm)	Sees* all particles of a few ~5 X 10^{-6} m (most cloud particles) and greater. No multiple scattering effects	Attenuation in moderate to heavy rainfall
cm wavelength (1-10 cm)	Less attenuated under heavy rain	Unable to see majority of cloud

* Depends also on volume concentration of particles; sees ice and water particles with almost equal sensivity

Range resolved systems

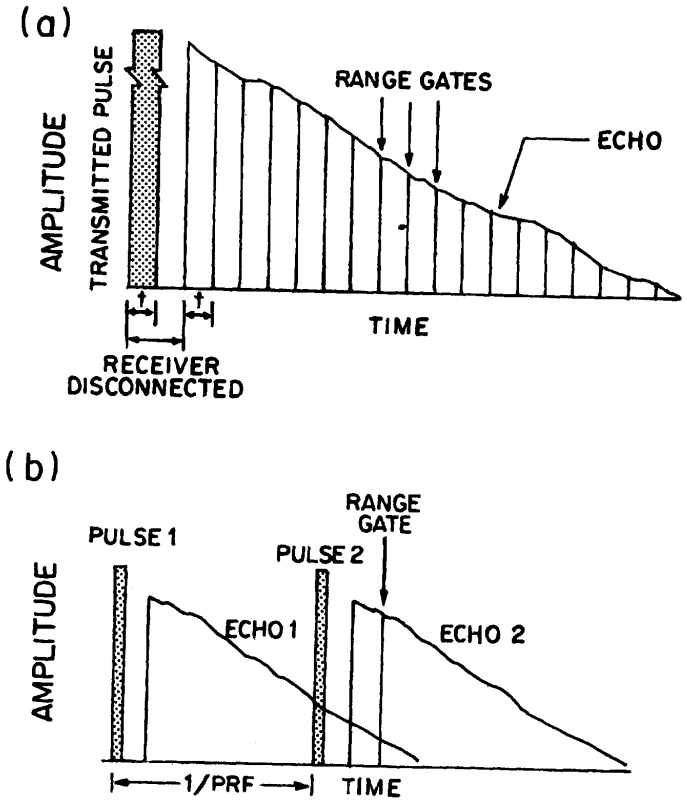

Pulsed systems

- finite pulse length h and echoes are spread along the path
- sampling at equally spaced times t establishes the range gating
- the volume of echoes are thus contained in a range element of h/2
- sampling period is thus $t \geq h/2c$ so sampling points are independent of each other

Pulses are transmitted at a rate known as the pulse repetition frequency (PRF)

$$PRF < \frac{c}{2R_{\max}}$$

Microwave Wavelengths:

$$f_{GHz} = \frac{30}{\lambda_{cm}}$$

10 cm ←→ 3 GHz (S-band)
5 cm←→6 Hz (C-band)
3 cm ←→ 10 GHz (X-band)
1.5 cm ←→ 20 GHz (K-band)
1 cm←→ 30 GHz (Ka-band)
3 mm ←→ 90 GHz (W-band)
2 mm ←→ 150 GHz (D-band)

CloudSat's collimating Antenna

Composite Graphite Antenna

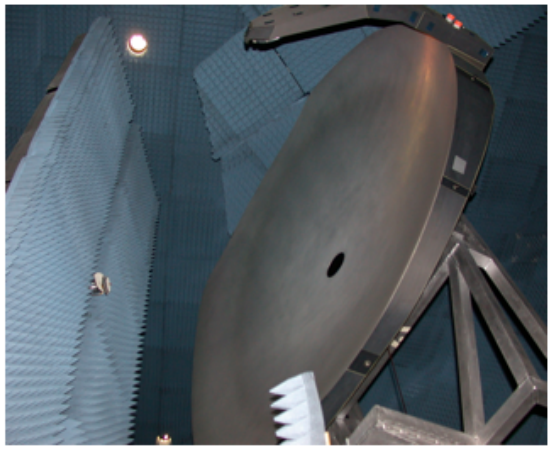

The 1.85 m Cloudsat antenna measured at 94 GHz on the cylindrical near-field scanner

- The challenge – maintain surface smoothness of a 1.85 m antenna
- The required rms surface accuracy of M1 is 50 μm (~ wavelength / 50)

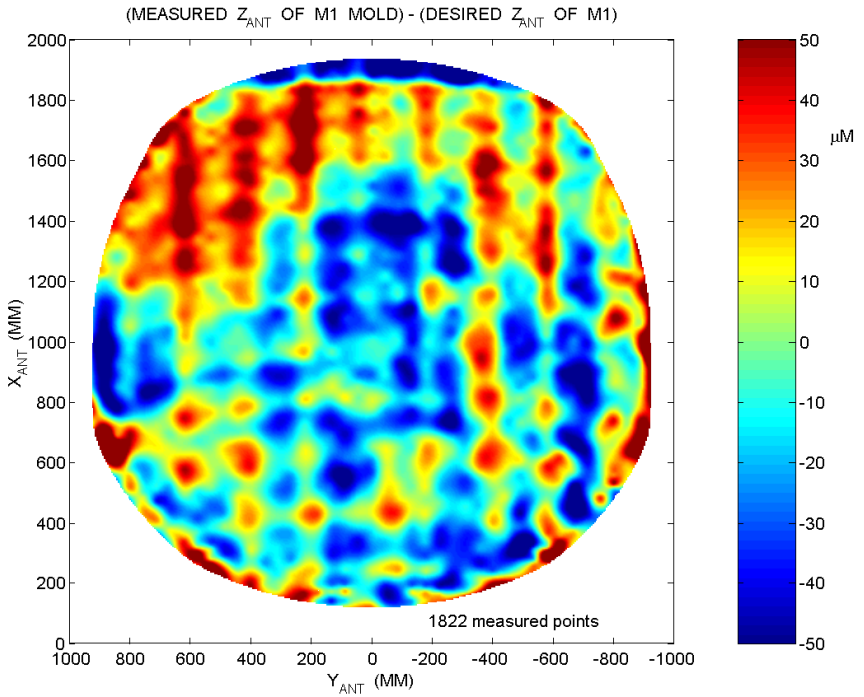

- Estimated ~27 μm of effective rms surface error based on analyses of mold.
- Final rms accuracy: ~5 μm

Sample Microwave Beam Pattern

29 GHz (1 cm) Feed-Horn

Antenna Gain G:
Defines the directionality of a beam.

$$G = \frac{I_p}{P_t / 4\pi R^2}$$

I_p: Actual Flux (W/m^2) crossing a unit area at R

$P_t / 4\pi R^2$: Flux from an isotropic emitter

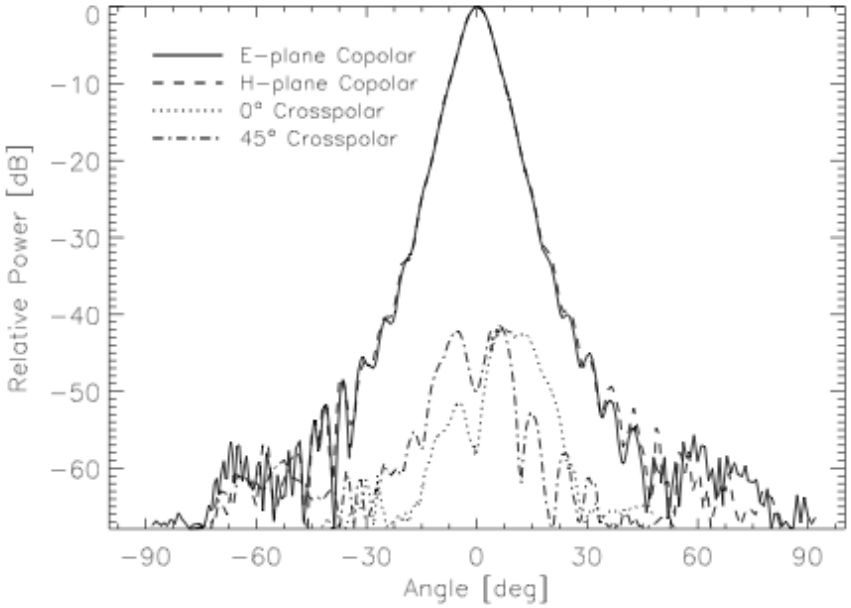

13 cm Wavelength feed horn

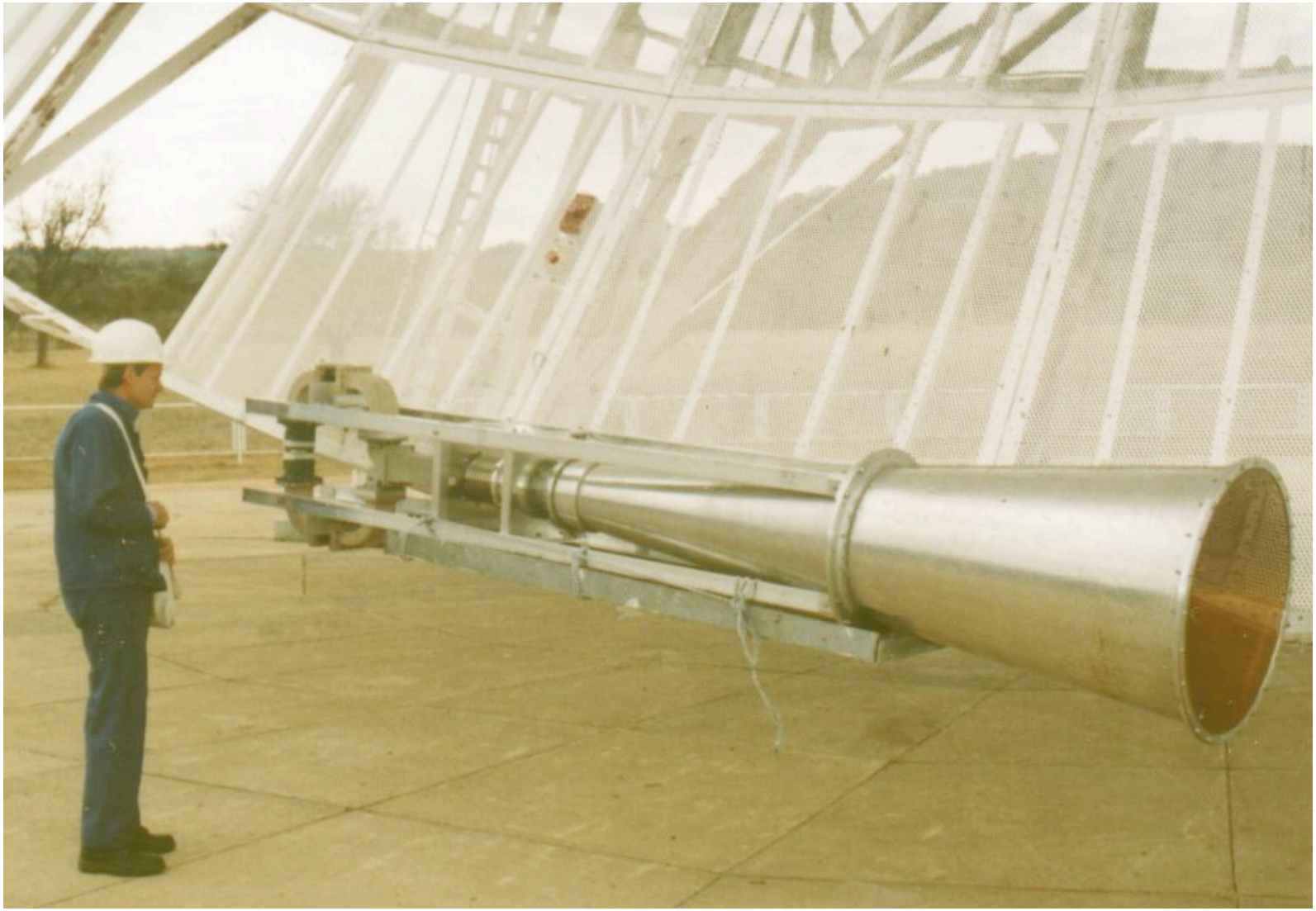

Radar Reflectivity

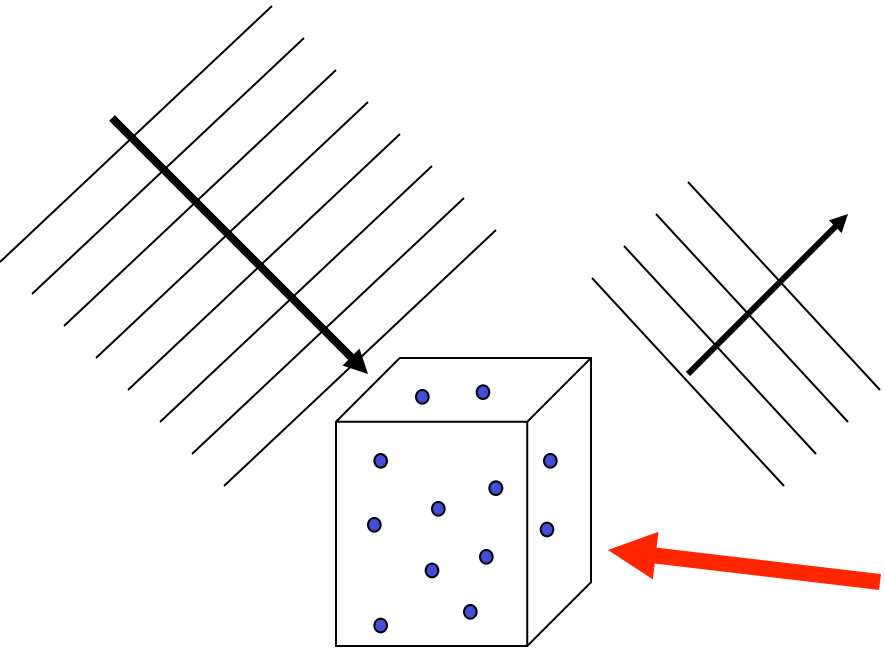

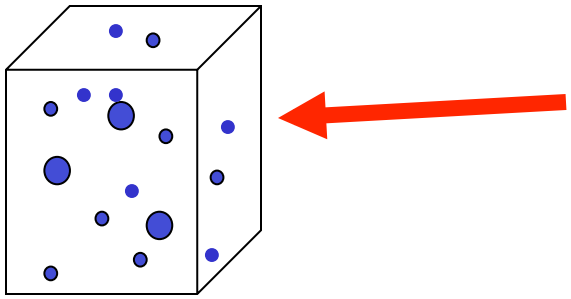

Power returned to radar after being scattered from cloud volume is related directly to size of particles in the volume

In atmospheric sciences, we express this returned power in terms of the quantity Z, the radar reflectivity

For a hypothetical cloud (particles all the same size), the power returned (or Z) is proportional to the square of the water and ice content (w) of the (radar) volume $\mathbf{Z = aw^2}$

BUT

For real clouds, particles in the volume range in size. The power returned (i.e. Z) is *approximately* proportional to the square of the water and ice content of the (radar) volume. The degree to which this proportionality exists varies from cloud type to cloud type. $\mathbf{Z \sim aw^b}$

Radar

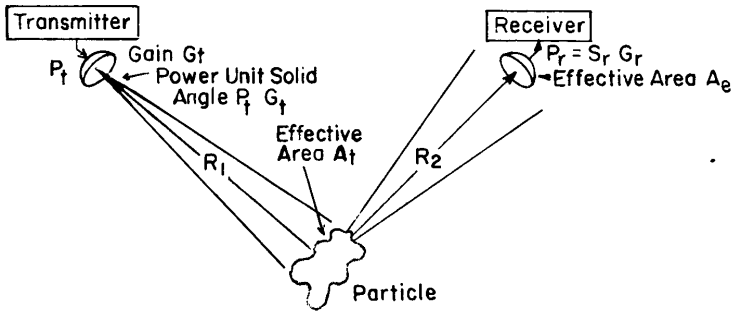

Energy incident on volume is defined by antenna gain

$$G = \frac{I_p}{P_t / 4\pi R^2}$$

$$P_{inc} = I_{inc} A_t = \frac{P_t G A_t}{4\pi R_1^2}$$

Basic scattering equation

Scattering from a particle of size r

$$I_{sca} = \frac{|S(\Theta)|^2 I_{inc}}{k^2 R_2^2} = \frac{I_{inc}\lambda^2}{R_2^2} C_s(r,\Theta)$$

for a volume dV of distributed particles

$$I_{sca} = \frac{I_{inc}\lambda^2}{R_2^2} dV \int n(r) C_s(r,\Theta) dr$$

# of particles per unit volume of size r

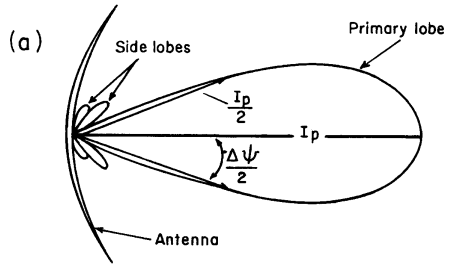

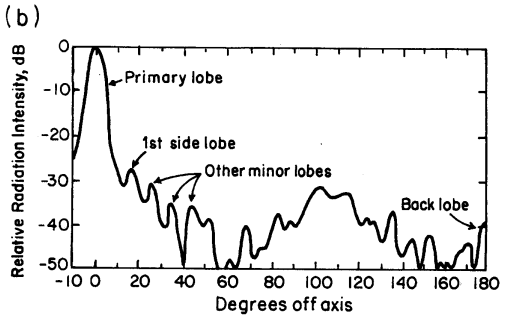

General form of radar equation (no attenuation)

$$P_r = I_{sca} A_e = \frac{I_{inc}\lambda^2}{R_2^2} dV \int n(r) C_s(r,\Theta) dr$$

$$P_r = \frac{P_t G \lambda^2}{4\pi R_1^2} \frac{A_e}{R_2^2} dV \int n(r) C_s(r,\Theta) dr$$

for monostatic systems

$$R_1 = R_2$$

$$A_e = G\lambda^2 / 4\pi$$

$$dV \approx R^2 \Delta\phi \Delta\varphi h / 2$$

$$\frac{P_r}{P_t} = \frac{G^2 \lambda^4}{(4\pi)^3 R^2} \frac{\Delta\phi \Delta\varphi h}{2} \int n(r) C_b(r) dr$$

$$Z \equiv \frac{\lambda^4}{\pi^5 \cdot 10^{-7} |K|^2} \int n(r) C_b(r) dr$$

Index of refraction of water (or ice) as function of λ

$$\frac{P_r}{P_t} = C \frac{|K|^2}{R^2} Z$$

Function of Instrument parameters: P_t, G, h, $\Delta\Phi$, $\Delta\varphi$ and λ

Function of Scatterers only. Units: $mm^6\ m^{-3}$

Radar equation (no attenuation): Rayleigh scattering

$$C_b(r) = \pi r^2 Q_s \left(\frac{2\pi r}{\lambda}\right) P(\Theta = 180°)$$

$$C_b(r) = \frac{8}{3}\frac{\pi D^2}{4}|K|^2\left(\frac{\pi D}{\lambda}\right)^4 \frac{3}{2}$$

$$C_b(r) = \frac{\pi^5}{\lambda^4}|K|^2 D^6$$

$$Z \equiv \frac{\lambda^4}{\pi^5 \cdot 10^{-7}|K|^2}\int n(r)C_b(r)dr$$

it follows that

$$Z = \int n(D)D^6 dD$$

This Z defined wrt to water

Weather radar (cm):
Z→ precipitation

mm radar:
Z → cloud water content
(liquid and/or ice)

Radar Reflectivity often expressed in dBZ
$dBZ = 10\log_{10}(Z)$

So a 50dBZ differential in reflectivity means 5 orders of magnitude

E.g. derived from 14 GHz TRMM radar MDS~19 dBZ

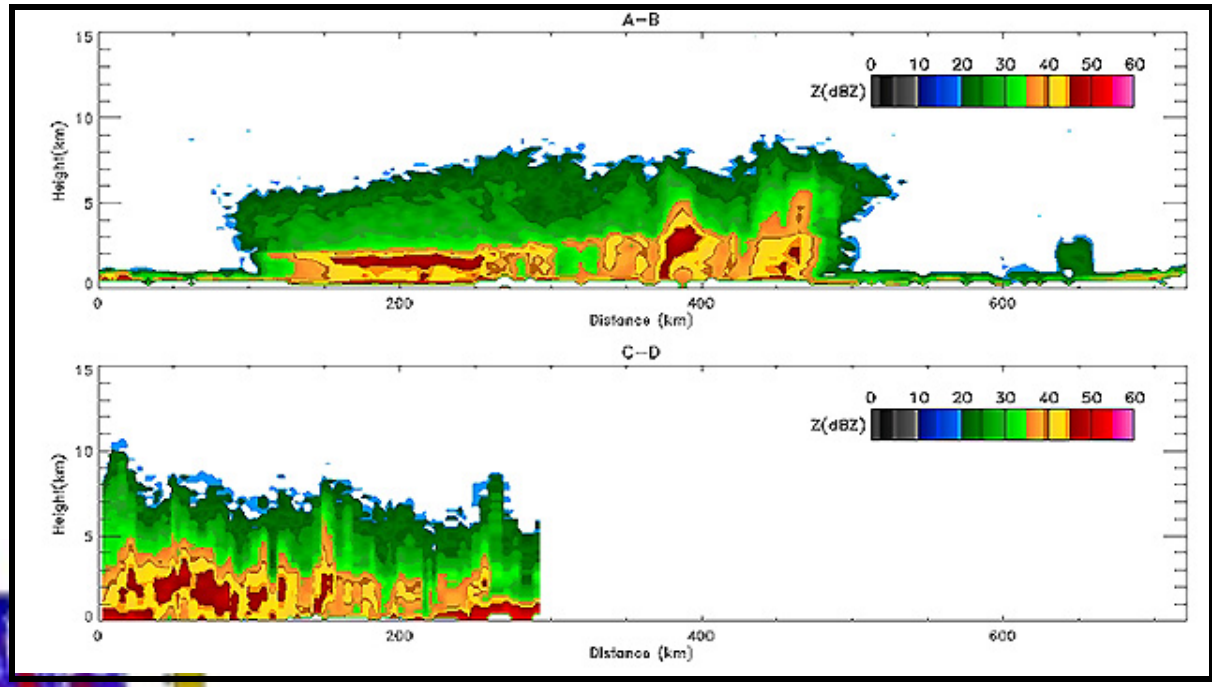

ice particles feeding precipitation

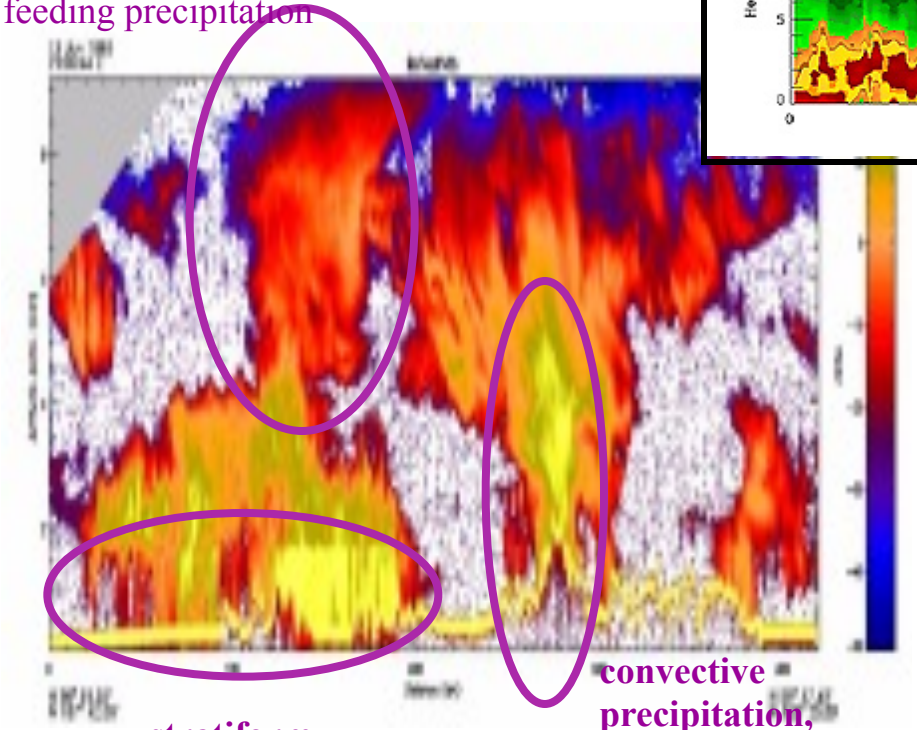

stratiform precipitation

convective precipitation, suggestion of hail

CloudSat 94 GHz radar- MDS~-30 dBZ

E.g. of DC8 airborne radar data

Z-R Relationship

Marshall Palmer Distribution:

$$n(D) = N_0 e^{-\Lambda D}$$

$$Z = N_0 \int_0^\infty e^{-\Lambda D} D^6 dD$$

$$Z = N_0 (6!) \Lambda^{-7}$$

$$R = \frac{1}{\rho} \int_0^\infty m(D) n(D) v(D) dD$$

$$R = \frac{\pi}{6} \rho N_0 \int_0^\infty D^3 e^{-\Lambda D} a D^b dD$$

$$R = \frac{\pi}{6} \rho N_0 a \frac{\Gamma(4+b)}{\Lambda^{4+b}}$$

$$Z = AR^B$$

$$Z \approx 200 R^{1.6}$$

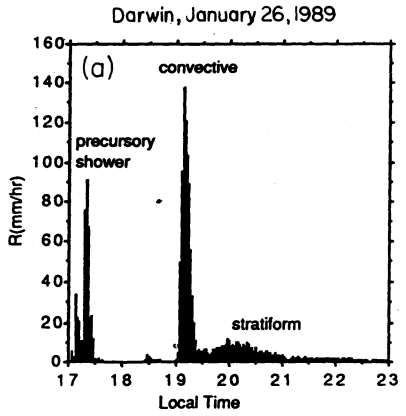

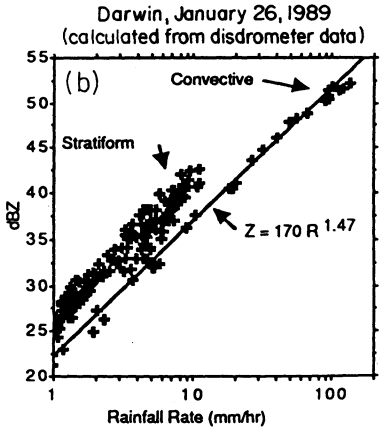

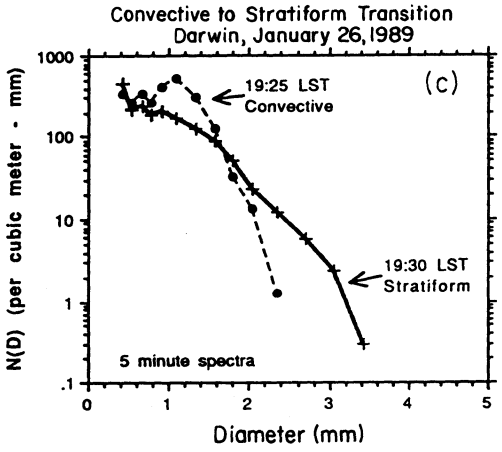

But: this relationship is dependent on the precise DSD

Z-Snow

Size Distribution ~ Exponential:

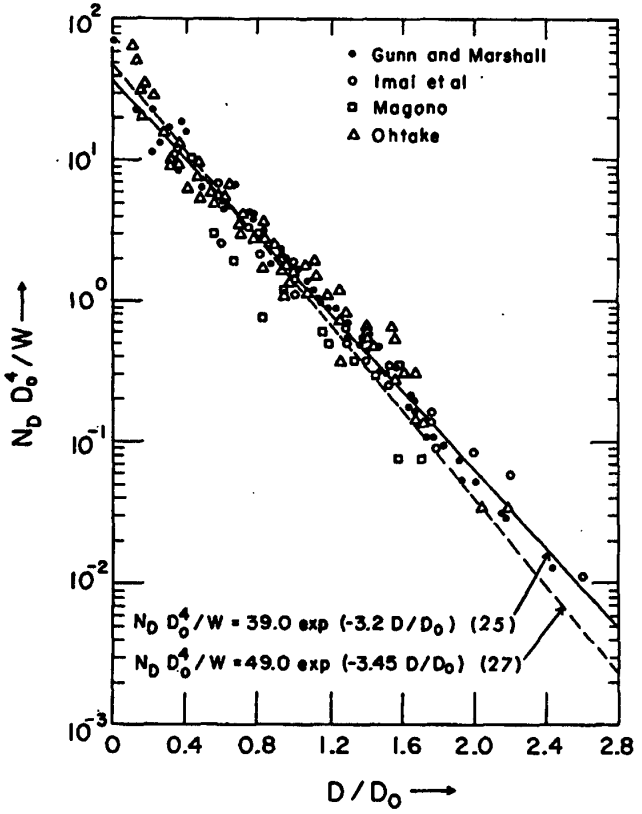

But we have a complication, snow might be regarded as a 'mixture' of water, ice and air

$$K_s = \frac{m_s^2 - 1}{m_s^2 + 2} = P_w \frac{m_w^2 - 1}{m_w^2 + 2} + P_i \frac{m_i^2 - 1}{m_i^2 + 2}$$

$$P_w \sim \rho_s^2$$

$$P_i \sim \rho_s (1 - \rho_s)/\rho_i$$

The 'effective' density of snow, ρ_s, is highly variable - for dry snow typically 0.02-0.06 g/cm3

TABLE I
COMPLEX REFRACTIVE INDICES OF DRY SNOW AT DIFFERENT MICROWAVE FREQUENCIES

	t = -10° C			t = -5° C		
ρ_s = 0.02 g/cm^3	0.04 g/cm^3	0.06 g/cm^3	0.02 g/cm^3	0.04 g/cm^3	0.06 g/cm^3	
GHz band						
34. (Ka)	1.01404+ *i*0.000085	1.02869+ *i*0.000342	1.04397+ *i*0.000773	1.01404+ *i*0.000075	1.02872+ *i*0.000308	1.04405+ *i*0.000679
17. (Ku)	1.01406+ *i*0.000048	1.02879+ *i*0.000192	1.04420+ *i*0.000434	1.01406+ *i*0.000041	1.02880+ *i*0.000163	1.04422+ *i*0.000369
9.3 (X)	1.01407+ *i*0.000027	1.02882+ *i*0.000108	1.04426+ *i*0.000244	1.01407+ *i*0.000023	1.02882+ *i*0.000091	1.04427+ *i*0.000206
5.4 (C)	1.01407+ *i*0.000016	1.02883+ *i*0.000066	1.04428+ *i*0.000148	1.01407+ *i*0.000014	1.02883+ *i*0.000055	1.04428+ *i*0.000125
2.9 (S)	1.01408+ *i*0.000009	1.02884+ *i*0.000034	1.04429+ *i*0.000077	1.01408+ *i*0.000007	1.02884+ *i*0.000029	1.04429+ *i*0.000065

Z-Snow

But we have a complication, snow might be regarded as a 'mixture' of water, ice and air

$$K_s = \frac{m_s^2 - 1}{m_s^2 + 2} = P_w \frac{m_w^2 - 1}{m_w^2 + 2} + P_i \frac{m_i^2 - 1}{m_i^2 + 2}$$

$$P_w \sim \rho_s^2$$

$$P_i \sim \rho_s (1 - \rho_s) / \rho_i$$

As with liquid precipitation;

$$Z_e \sim AS^b$$

(dry snow)

TABLE II

COEFFICIENTS IN Z_e—R RELATIONSHIPS FOR SNOWFALLS AT DIFFERENT MICROWAVE FREQUENCIES

		2.9 GHz *S*-band	5.4 GHz *C*-band	9.3 GHz *X*-band	17. GHz *Ku*-band	34. GHz *Ka*-band	Rayleigh dry snow	Rayleigh melted snow
snowflake density ρ_s g/cm^3								
0.02	*A*	870.	690.	410.	130.	10.0	950.	1950.
	b	2.01	1.90	1.60	1.00	0.50	2.03	2.22
0.04	*A*	570.	510.	340.	160.	20.0	610.	1950.
	b	2.01	1.95	1.75	1.20	0.61	2.03	2.22
0.06	*A*	460.	420.	240.	170.	28.0	490.	1950.
	b	2.02	1.98	1.95	1.35	0.95	2.03	2.22

mm-wave Z and cloud water/ ice water content

Z- Ice water content relationships

At mm wavelengths (& for non-Rayleigh scatterers, e.g. ice crystals, precipitation)

$$Z = \int \frac{|K|^2}{0.93} n(D) D^6 f(D) dD$$

f(D) is a Rayleigh-to-Mie correction factor

0.93 = value of $|K|^2$ for water at cm wavelengths

($|K|^2$ = 0.686 at $0^{\circ}C$ at 94 GHz)

For the same reasons, there is not a one-to-one relation between cloud water and ice contents and mm wave radar reflectivity

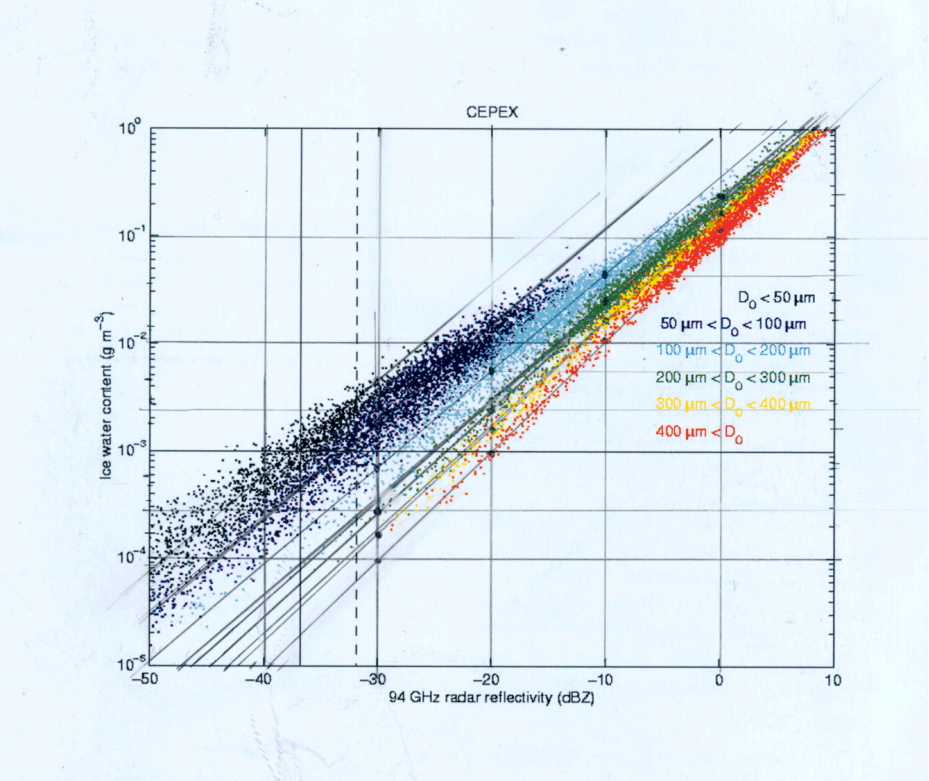

Radar equation with Attenuation

$$P_r = C\frac{|K|^2}{R^2}Z \quad \exp\left(-2\int_0^R \sigma_{ext}(R')\,dR'\right)$$

Attenuation

Radar signals are attenuated by atmospheric gases, cloud particles, and precipitation.

$$\sigma_{ext}^{D} = \sigma_{gas}^{D} + k_c w + k_p R^{\gamma} \qquad \text{(usually expressed in dB/km)}$$

Gases: O_2, H_2O | Cloud water | Precip

Attenuation by Gases

At microwave wavelengths, attenuation by gases is solely due to absorption by water vapor and molecular oxygen:

$$\sigma^D_{gas} = \sigma^D_{H_2O} + \sigma^D_{O_2}$$

Water Vapor (22 GHz):

$$\sigma^D_{H_2O} = 2f^2\rho_v\left(\frac{300}{T}\right)^{1.5}\gamma_1\left[\frac{300}{T}e^{-644/T}\frac{1}{\left(494.4-f^2\right)^2+4f^2\gamma_1^2}+1.2\text{x}10^{-6}\right]\ (dB/km)$$

$$\gamma_1 = 2.85\left(\frac{P}{1013}\right)\left(\frac{300}{T}\right)^{0.626}\ (GHz)$$

- f in GHz
- T in K
- P in hPa

Oxygen (60 GHz):

$$\sigma^D_{O_2} = 0.011f^2\left(\frac{P}{1013}\right)\left(\frac{300}{T}\right)^2\gamma\left[\frac{1}{(f-60)^2+\gamma^2}+\frac{1}{f^2+\gamma^2}\right](dB/km)$$

$$\gamma = \gamma_0\left(\frac{P}{1013}\right)\left(\frac{300}{T}\right)^{0.85}\ (dB/km)$$

(From Ulaby et al (1981).)

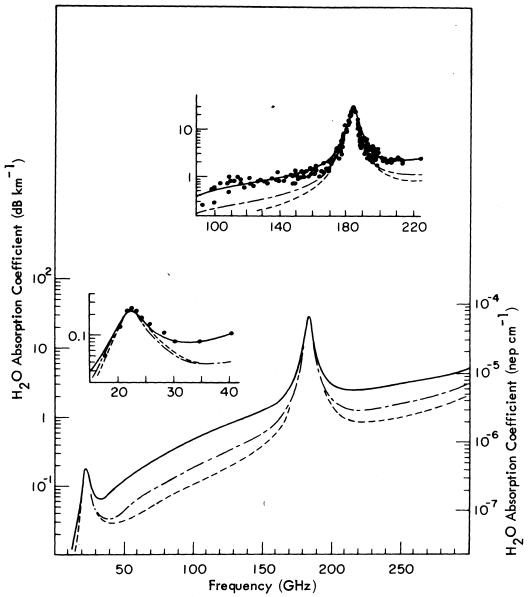

Fig. 5.5 Measured and calculated water-vapor absorption (from Waters, 1976). Calculations are shown for the Van Vleck–Weisskopf line shape (---), the Gross line shape (— · —), and the Gross line shape with the added empirical correction discussed in the text (—), with T=300 K, P=1013 mbar, and ρ_v=7.5 g m^{-3}. Points in the 20–40-GHz inset are measurements of Becker and Autler (1946), where T=318 K, P=1013 mbar, and ρ_v=10 g m^{-3}. Points in the 100–200-GHz inset are measurements quoted by Dryagin et al. (1966), where T=300 K, P=1013 mbar, and ρ_v=7.5 g m^{-3}.

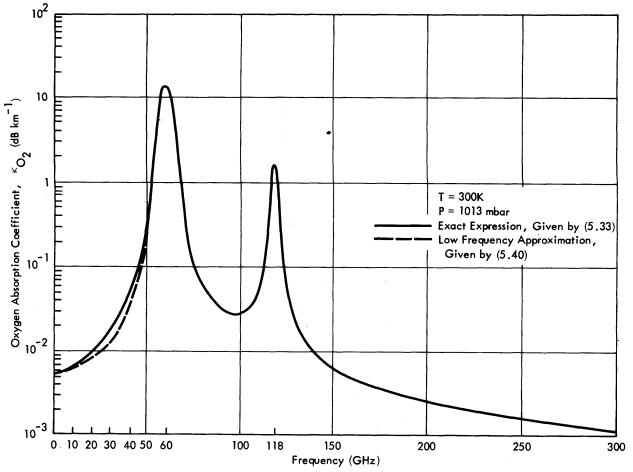

Fig. 5.6 Calculated oxygen absorption for sea-level conditions. The dashed curve is based on the low-frequency approximation given by (5.40).

Examples: S-band Radar (10 cm) $\sigma_{gas}^{D} = 0.0069 \ dB/km$
TRMM PR (14 GHz) $\sigma_{gas}^{D} = 0.0281 \ dB/km$
CloudSat CPR (94 GHz) $\sigma_{gas}^{D} = 0.5281 \ dB/km$

at p=1013 mb, T=300K, and $\rho_v = 7.5 \ g/m^3$

Attenuation by Cloud Particles

To estimate attenuation by cloud particles we invoke the Rayleigh approximation, since the radar wavelengths are much longer than the radii of typical cloud particles:

- absorption dominates since it is proportional to size parameter while scattering is proportional to size parameter to the fourth power

- $Q_{ext} \approx Q_{abs} = -4\chi \, \mathrm{Im}(K)$

$$\sigma_c^D = k_c w = -\frac{10}{\ln 10} \frac{6\pi}{\rho_L \lambda} \mathrm{Im}(K) w \ \left(dB/km\right)$$

Liquid	10 cm = 3 GHz			14 GHz			94 GHz		
	-8 C	10 C	20 C	-8 C	10 C	20 C	-8 C	10 C	20 C
n	8.94	9.02	8.88	5.39	6.89	7.44	2.53	3.04	3.34
k	1.8	0.9	0.63	3.03	2.78	2.41	1.23	1.75	2.04
Im(-K)	0.013	0.0069	0.0051	0.063	0.035	0.027	0.217	0.177	0.153
kc*	0.011	0.0056	0.0042	0.239	0.135	0.102	5.72	4.68	4.05
*In dB/km/g/m^3.									

- attenuation by ice particles is negligible since they have extremely small imaginary refractive indices
- liquid particles are negligible for weather radar but become important at high frequency

Ice (-20 C)	10 cm	14 GHz	94 GHz
n	1.78	1.78	1.78
k	0.0002	0.0007	0.003
Im(-K)	9.00E-05	0.0003	0.001
kc*	7.00E-05	0.0011	0.029
*In dB/km/g/m^3.			

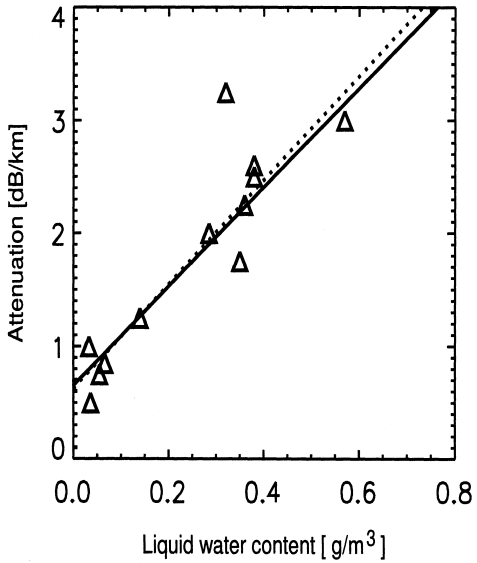

Data from University of Wyoming 95 GHz cloud radar in marine stratus off the coast of Oregon. (Vali and Haimov (1998)).

Figure 5. Linear fit of measured attenuation (dotted line, 0.62+4.6*LWC) and Liebe et al [6] model (solid line, 0.65+4.4*LWC).

Attenuation by Precipitation

Attenuation by precipitating particles is most often parameterized in terms of rainfall rate, R, using semi-empirical expressions.

$$\sigma_p^D = k_p R^\gamma = cZ^d \ \left(dB/km\right)$$

Rain	3 GHz	14 GHz	94 GHz
kp	4E-06	0.014	0.744
gamma	1	1.21	0.734
c	0.00003	0.0003	0.012
d	0.62	0.755	1.163

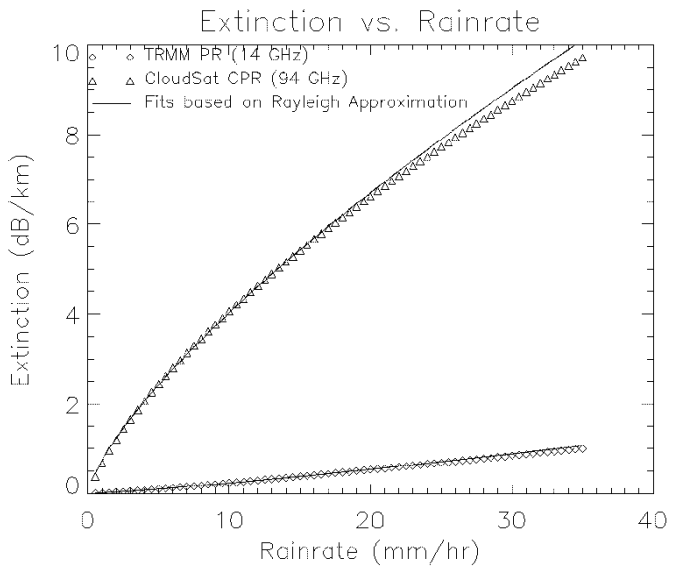

- Attenuation is small at S-band except in heavy rain
- At 10 GHz and higher, attenuation becomes significant
- Parameterization of attenuation by rainfall is a large source of uncertainty in retrievals due to their sensitivity to drop size distribution (DSD), particle shape, the presence of mixed-phase particles, and non-Rayleigh effects (above 10 GHz)

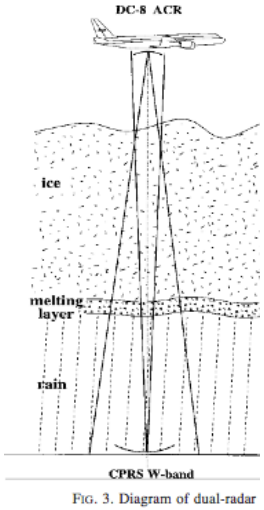

FIG. 3. Diagram of dual-radar

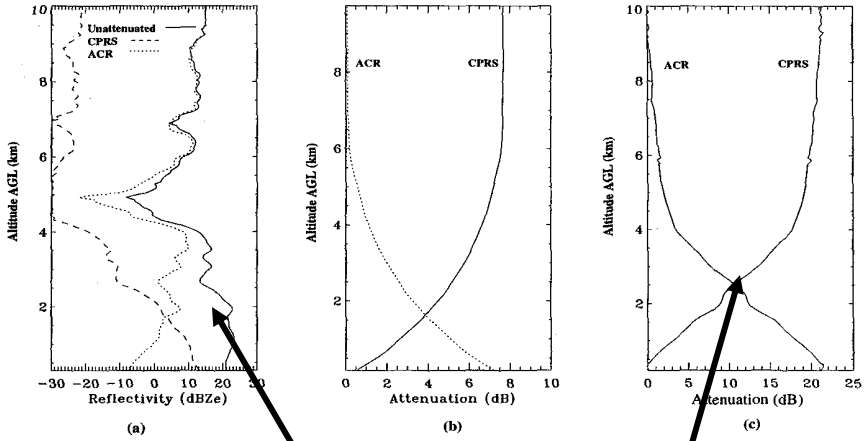

Reconstructed unattenuated reflectivity

Precip attenuation

Observed Precip attenuation at 94 GHz

Li et al., 2000

T' storm over Kansas

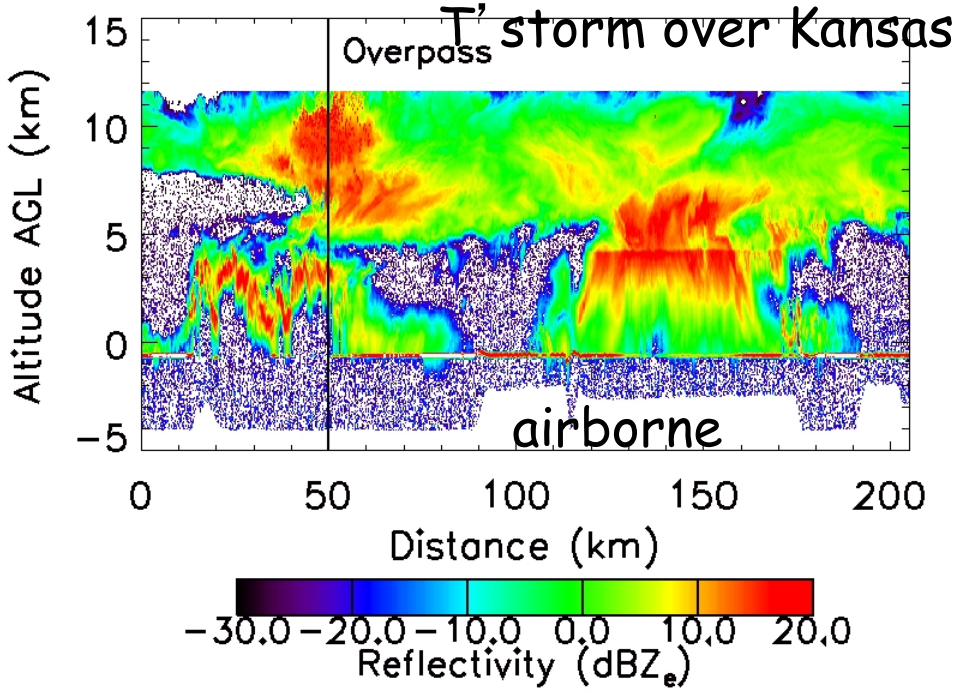

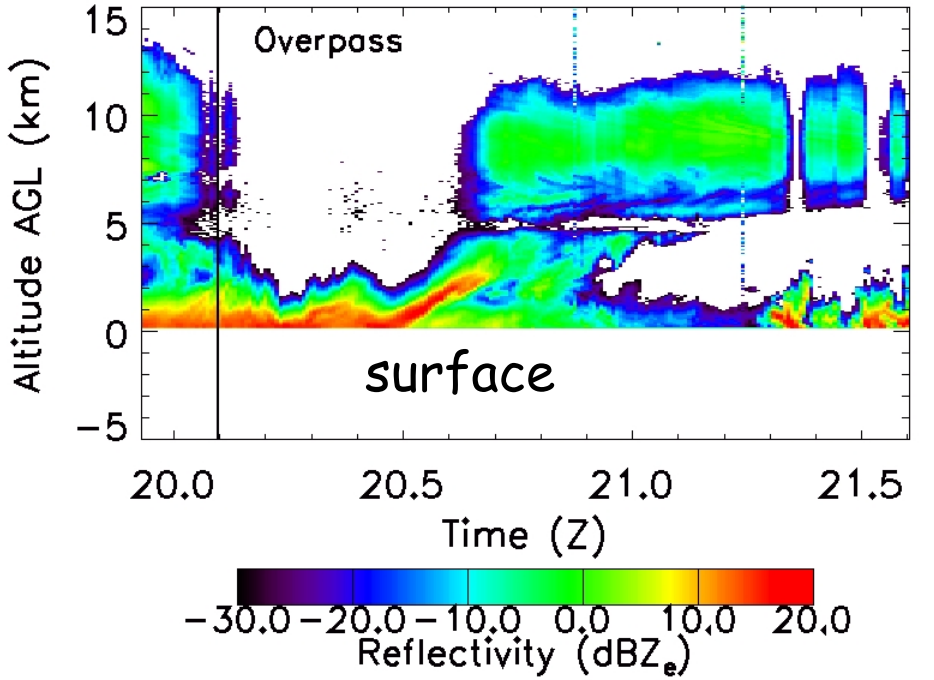

TRMM PR VS. CLOUDSAT CPR

PR: 14 GHz
CPR: 94 GHz

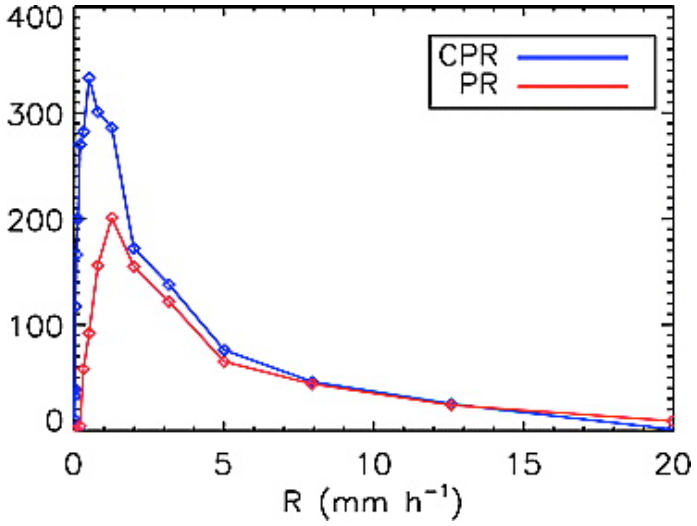

In project 5 you will investigate rain from TRMM PR vs. CloudSat

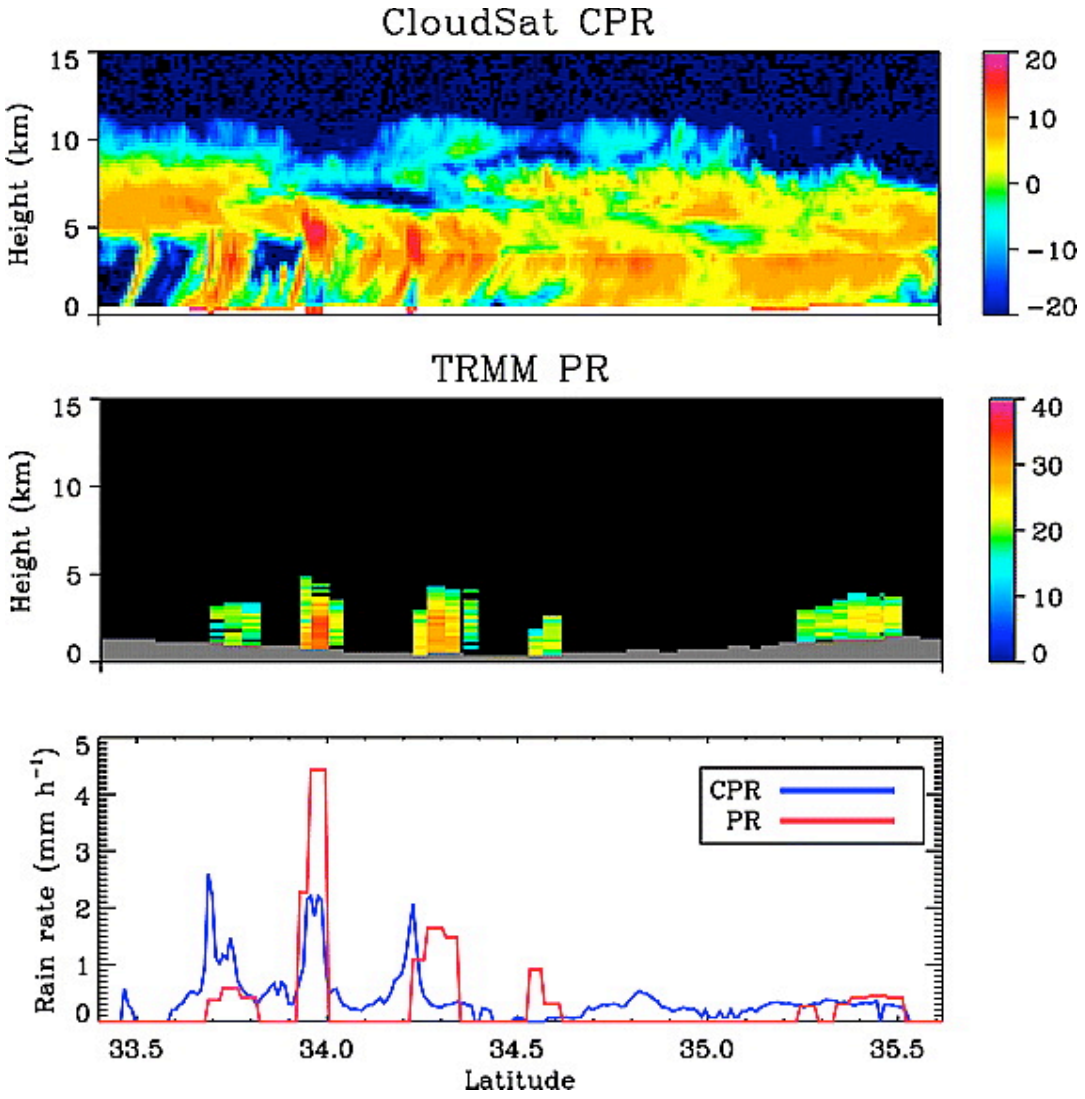

Haynes et al. (2009)

Example of 14, 94 GHZ radar Precipitation retrievals and effects of attenuation

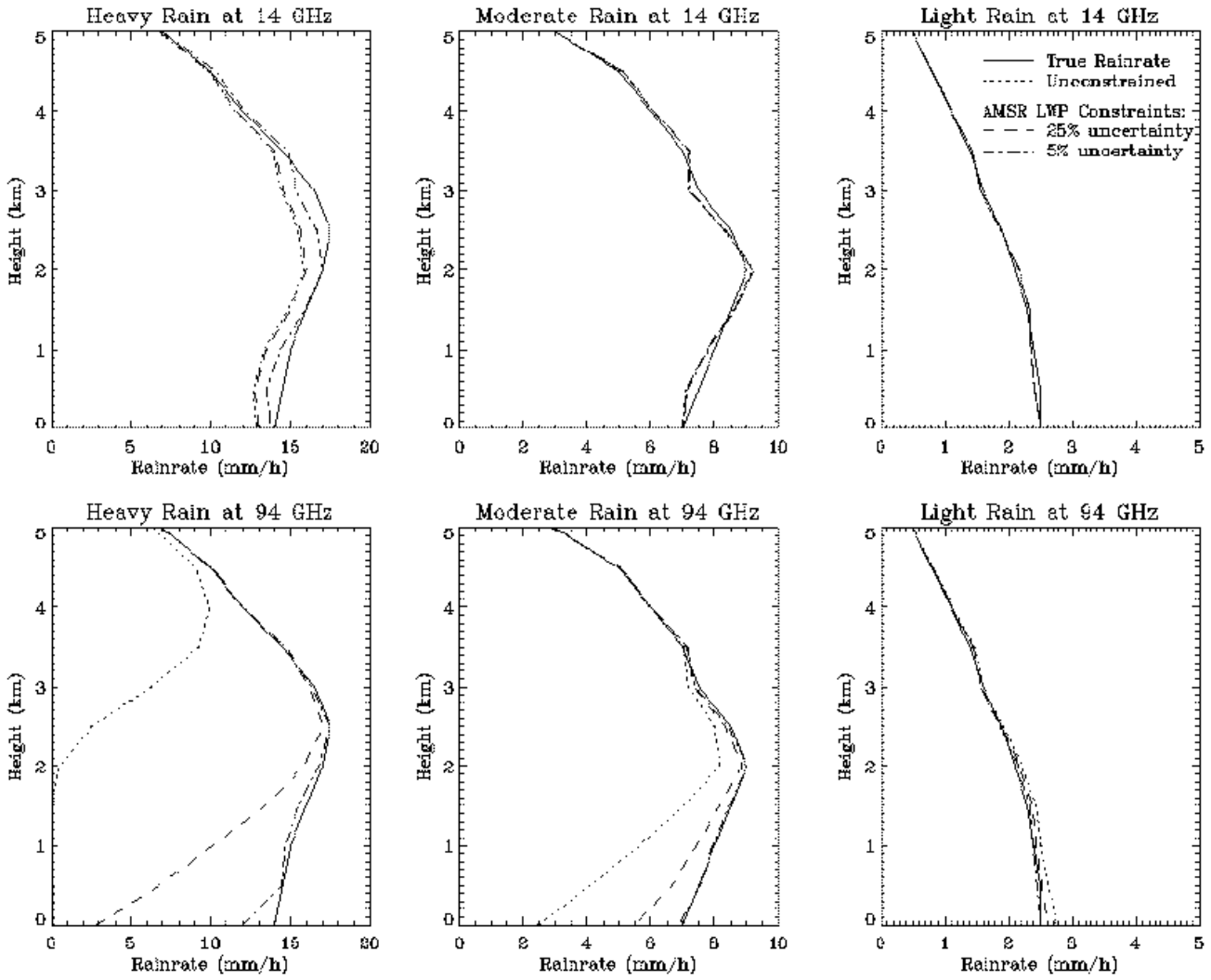

CloudSat: Rain detection more robust through "Path-Integrated Attenuation"

- PIA good to +/- 1 dB over ocean
- Minimum detectable rain-rate is 0.02-0.05 mm/hr
- Represents an average RR through the raining column
- In project 5 you will investigate this method vs. a more traditional method

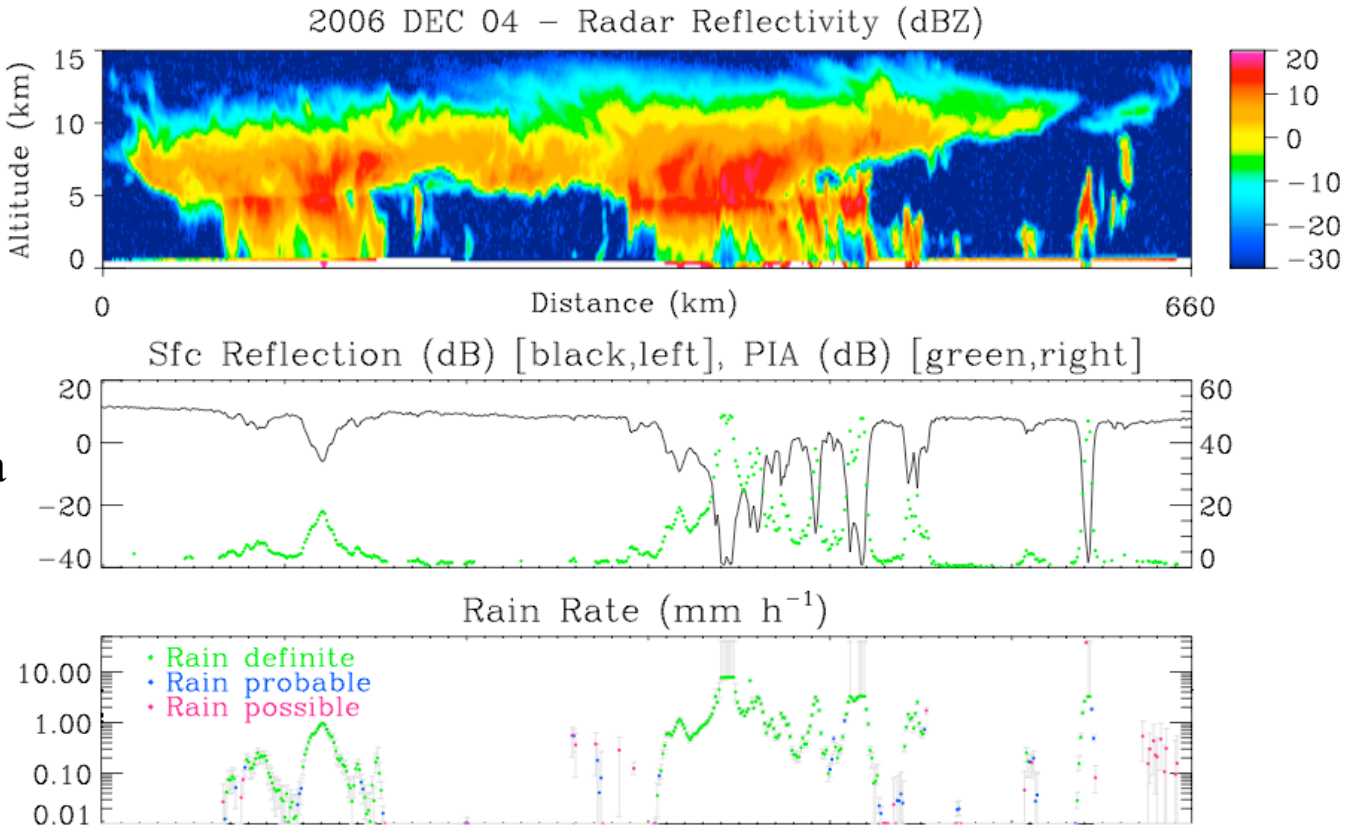

Figure 9. (top) An example of the CPR cross section through a precipitating system over the ocean, also illustrating (middle) the surface reflectivity and derived path attenuation and (bottom) the rain categorization.

CloudSat detected much more rain at high latitudes than previous estimates

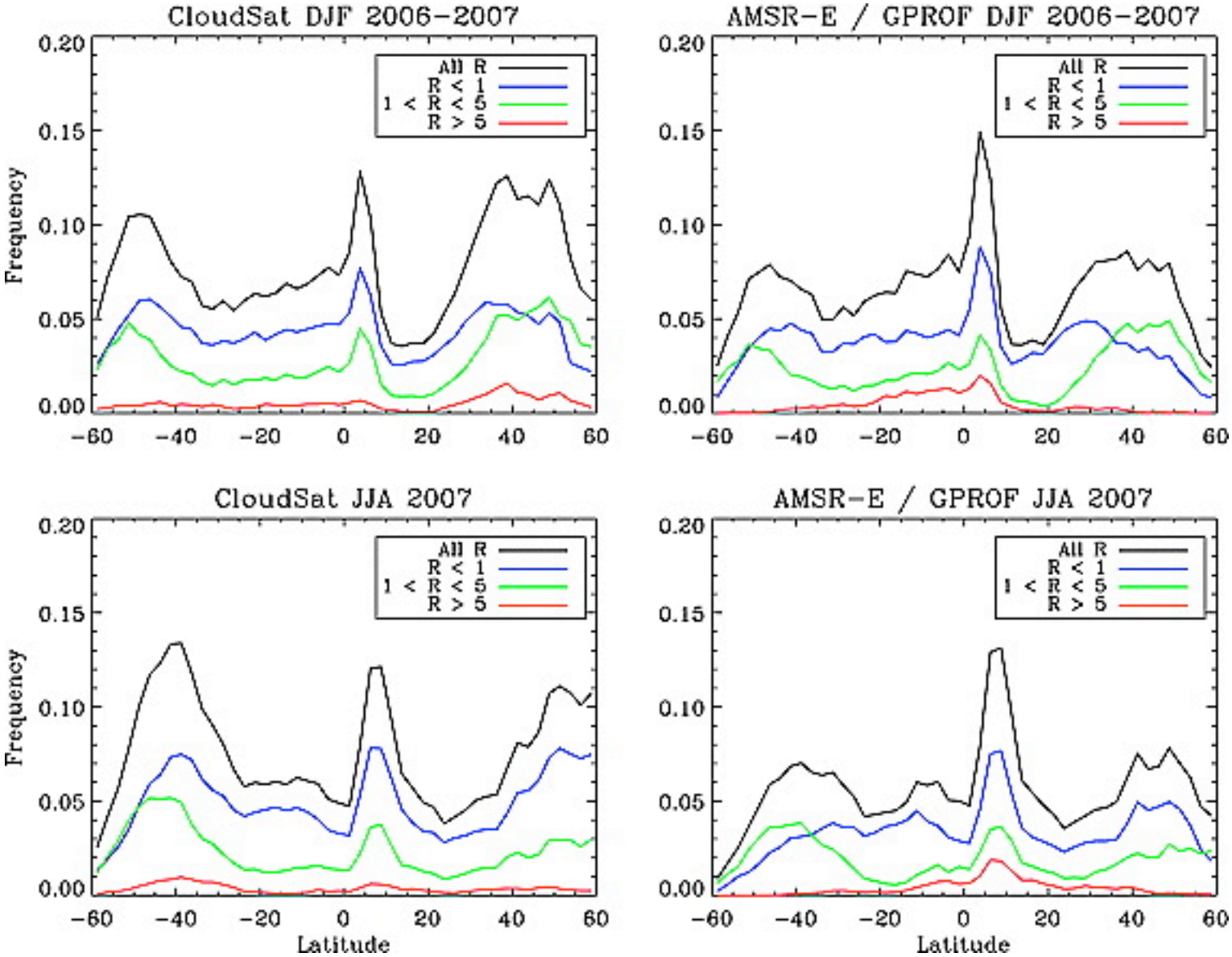

CloudSat detected more cloud ice than seen in previous observations and present in models

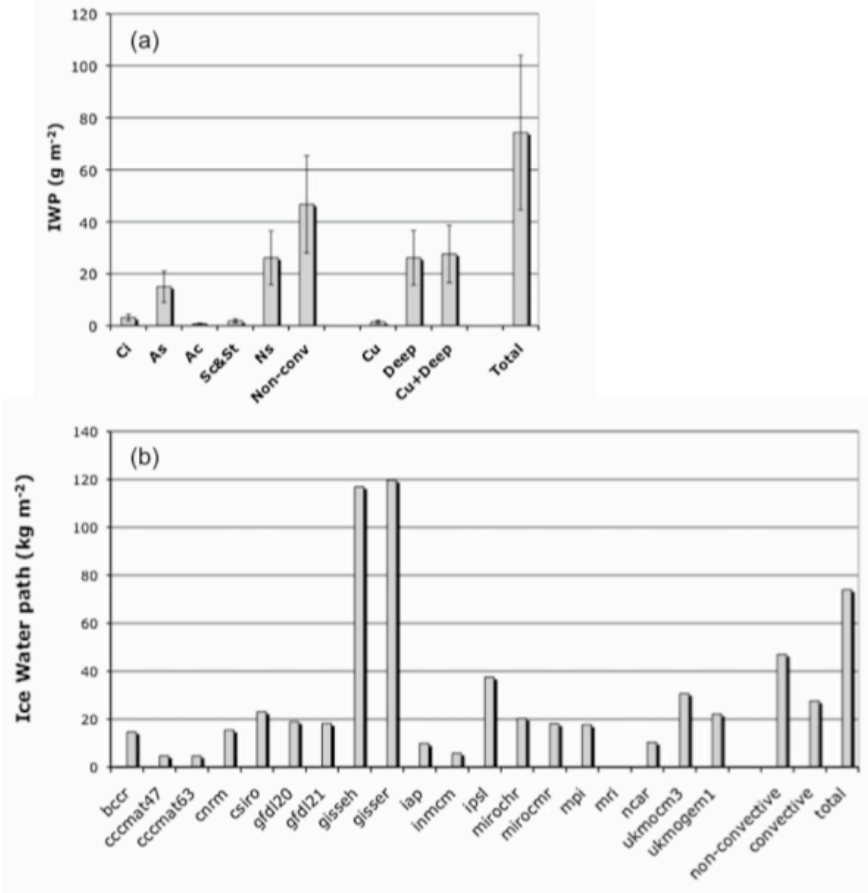

Figure 13. (a) Global mean ice water path calculated from Release 4 (R04) of the CloudSat 2B-CWC-RO product over the period 2006-12-01 to 2007-11-30. Ice water path is assigned to cloud types using the 2B-CLDCLASS product. "Convective" cloud refers to the sum of 2B-CLDCLASS cumulus and deep convection types; "nonconvective" includes the remaining types. Error bars indicate the estimated systematic uncertainties. (b) The global mean ice water path derived from 19 Intergovernmental Panel on Climate Change (IPCC) climate models from the 1970–1994 period of the 20th century GCM simulations contributed to the IPCC 4th Assessment Report (20c3m scenario) compared to the CloudSat observations of nonconvective, convective, and total repeated from Figure 13a.

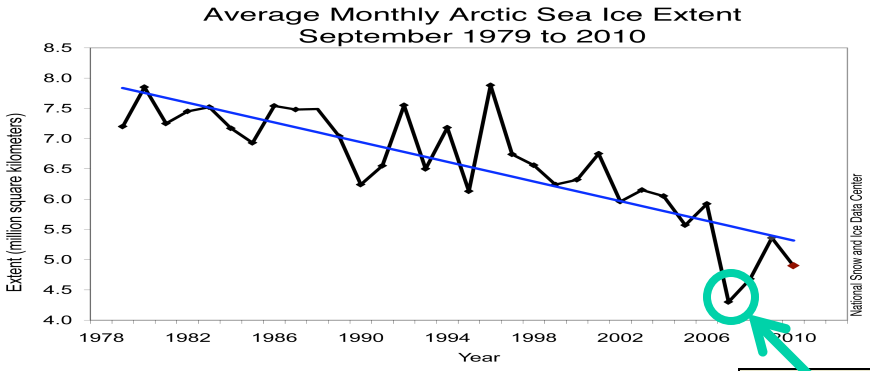

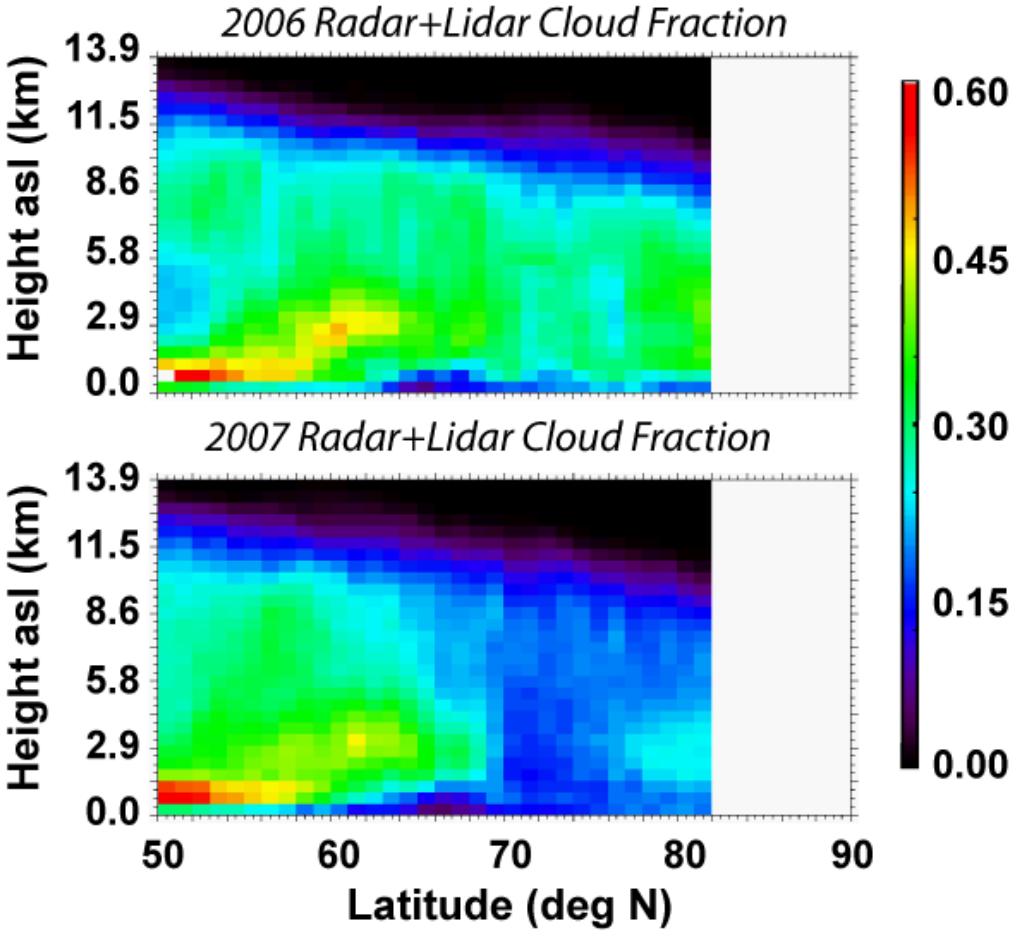

• 2007 arctic cloud reductions associated with anomalous weather patterns.

The increase in sunshine could melt 0.3 meters of ice or warm the surface ocean by 2.4 degrees Kelvin.

Kay et al. (2007)

Multi-parameter Radar

(ii) Dual polarization

$$P_{R,V/H} = \begin{bmatrix} P_{H,V/H} \\ P_{V,V/H} \\ P_U \\ P_v \end{bmatrix}$$

In principle, there are 16 different returned power parameters; in practice, two are typical used in a dual polarization radar:

ZDR & P_{HH}

$$ZDR = 10\log\frac{P_{HH}}{P_{VV}}$$

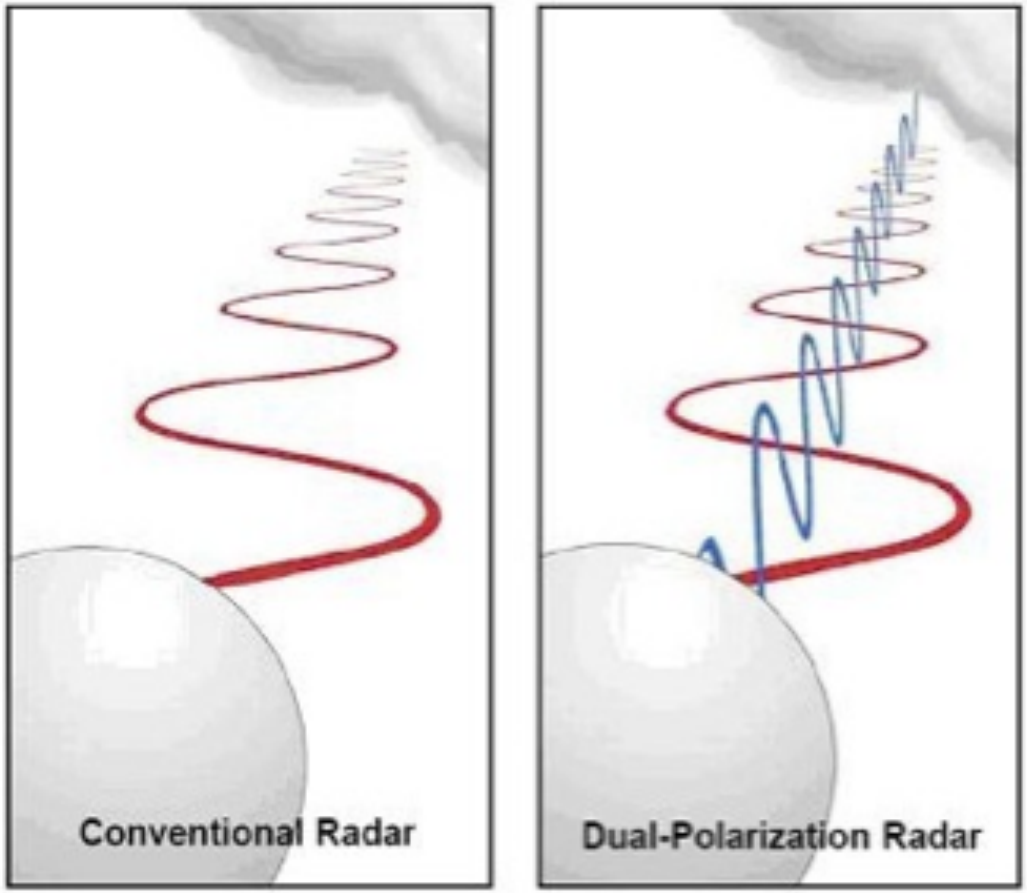

Dual-Pol Offers 4 Primary Parameters:

- Z
- Z_{DR}
- CC
- KDP

Upgrades completed to ~ 150 NWS radars to Dual-Pol in June 2013

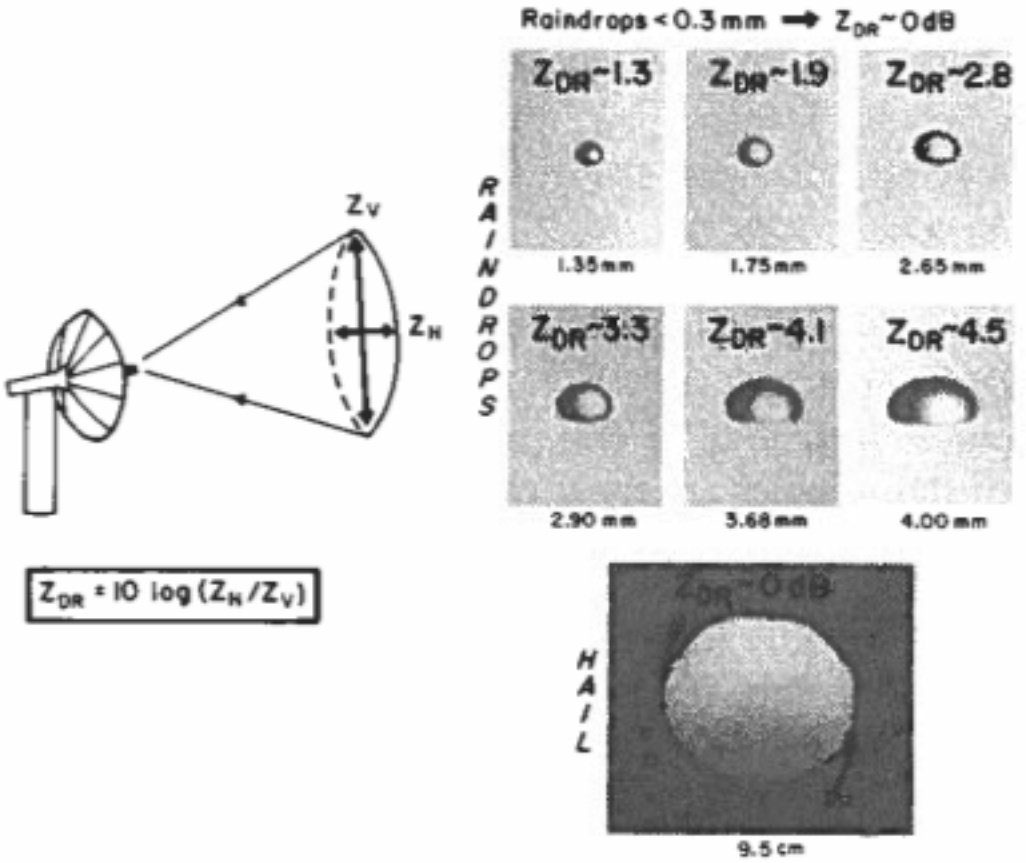

Figure 5.31 Summary of typical Z_{DR} values for raindrops of various sizes and hail. The black arrows on the hail represent its tumbling motions as it falls. Sizes are the median volume diameter (from Wakimoto and Bringi, 1988).

Polarimatric methods for measuring rainfall

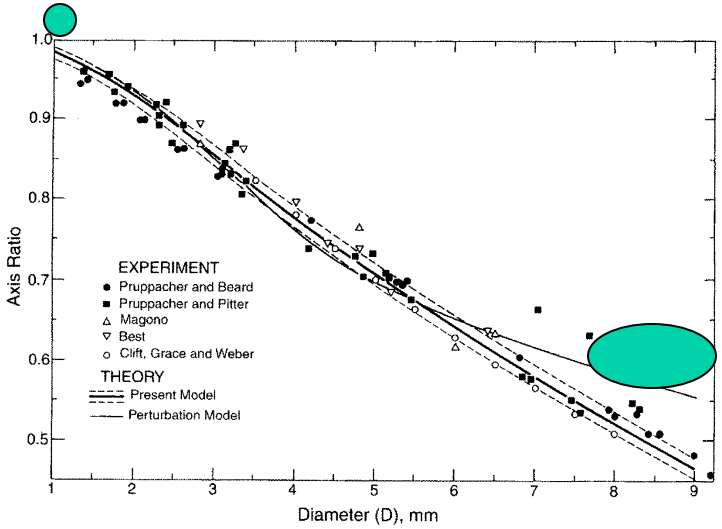

Oblateness of raindrop is related to rain-drop size

$$\Lambda = 2.6\, ZDR^{-0.63}$$

$$Z = N_0(6!)\Lambda^{-7}$$

$$R = \frac{\pi}{6}\rho N_0 a \frac{\Gamma(4+b)}{\Lambda^{4+b}}$$

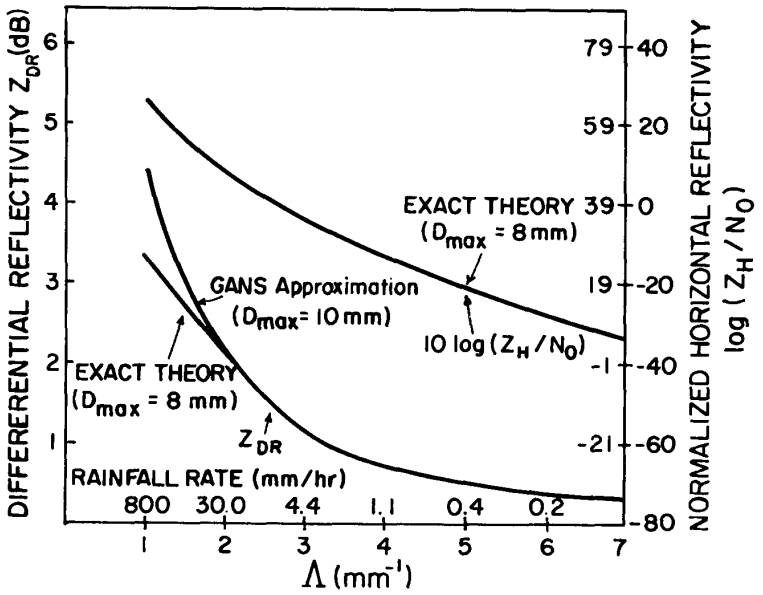

By measuring ZDR & Z, you can get R with fewer assumptions than with Z alone.

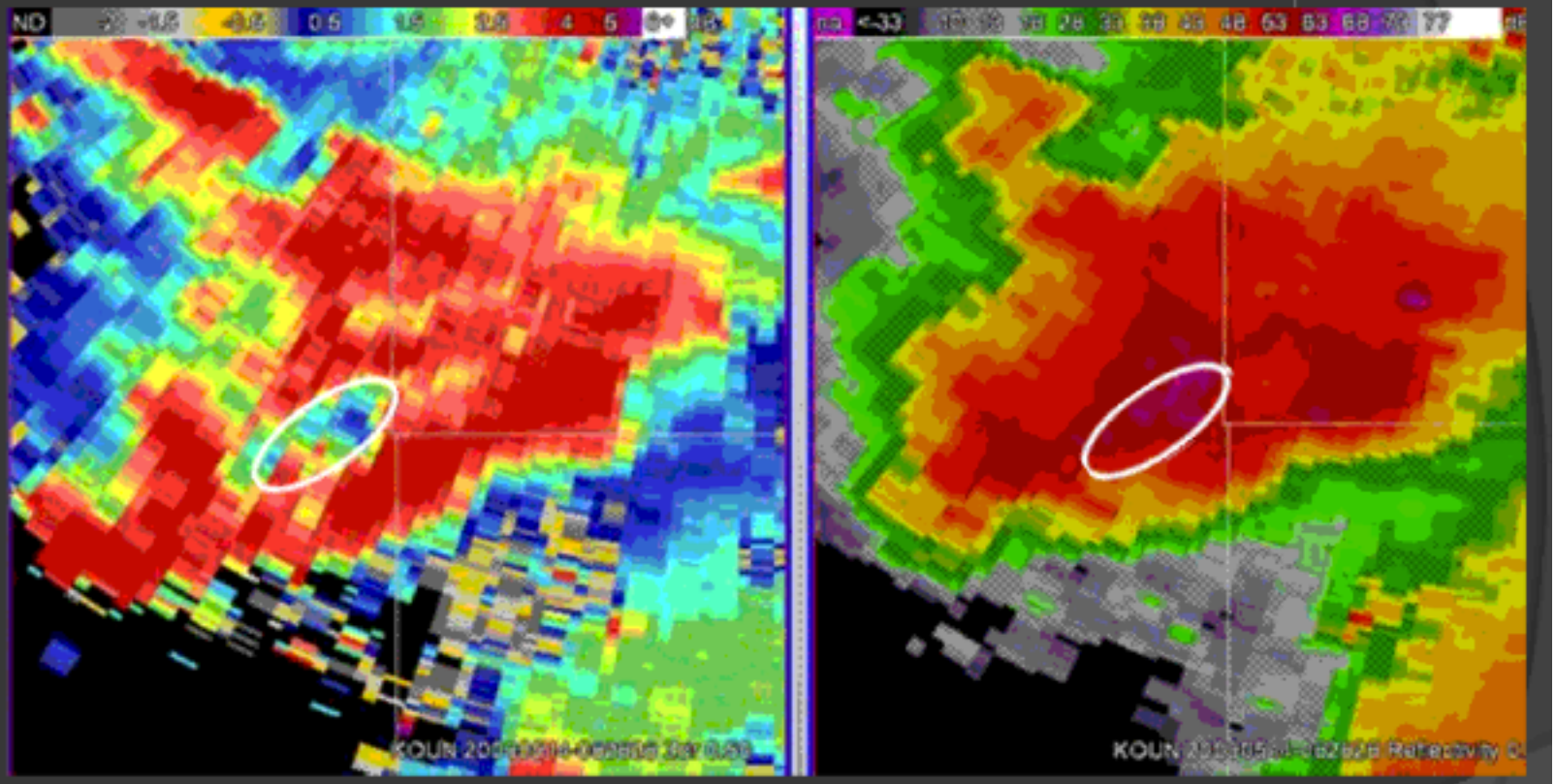

Differential Reflectivity (ZDR)

Reflectivity (Z)

The new differential reflectivity product will allow to more closely pinpoint location of largest hail in supercells (areas of ZDR near zero)

Phase Discrimination Via ZDR & Z

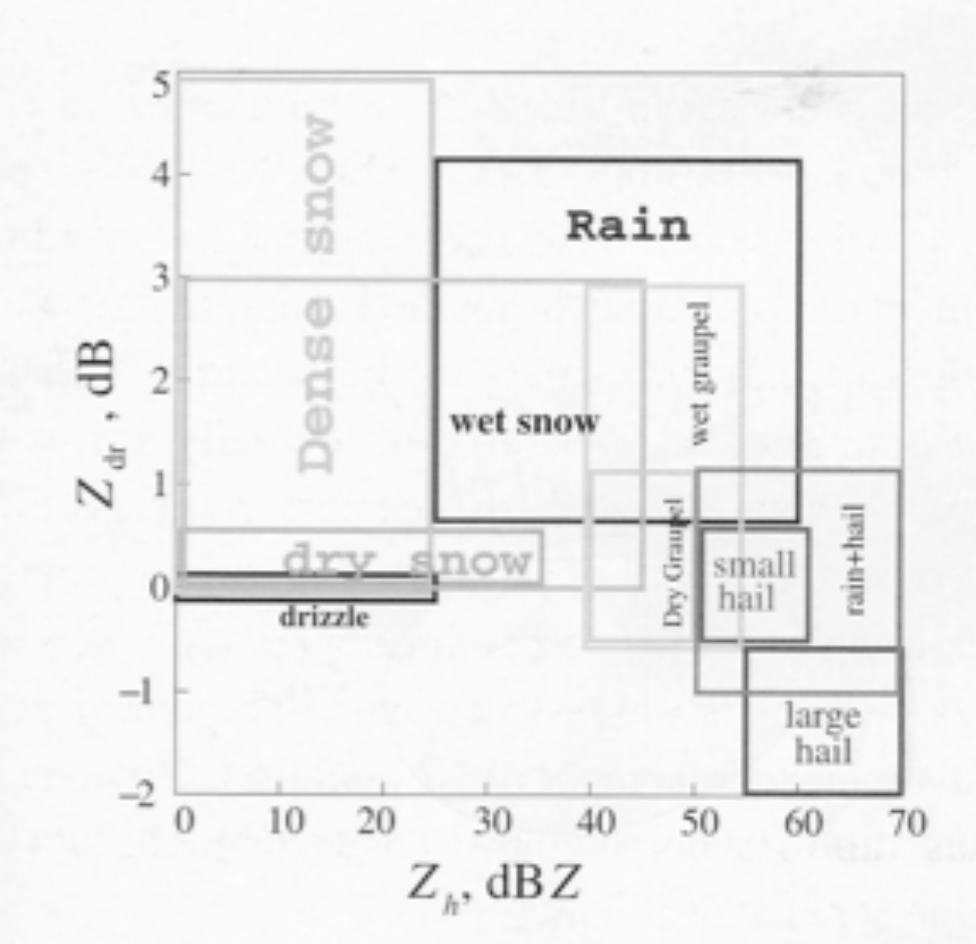

ZDR & Z can give you a reasonable guess on phase too!

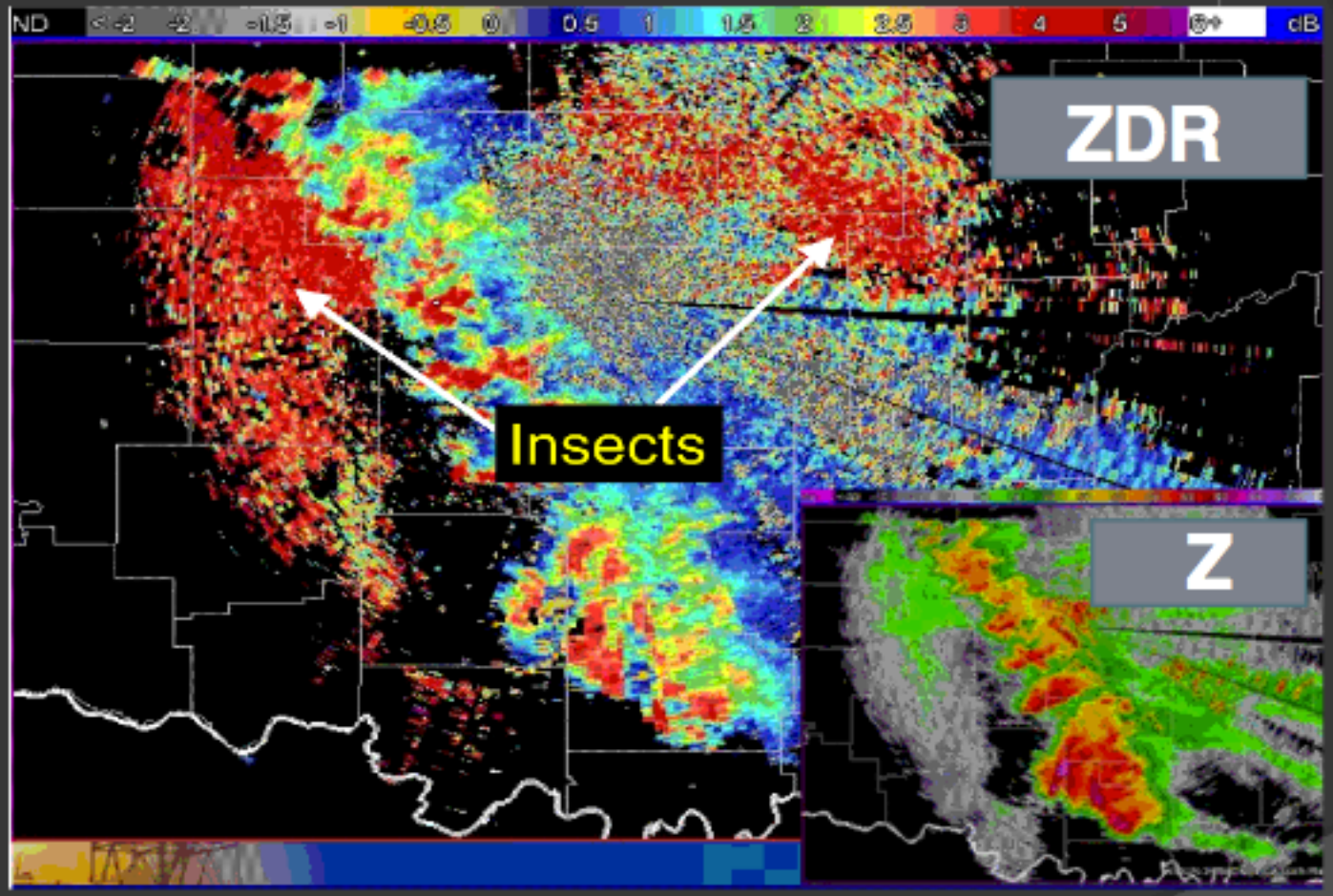

Note the area of low reflectivity (Z) coincides with high values of differential reflectivity (ZR). Insects are less reflective than precipitation targets and usually have more horizontal extent than vertical when flying through the air.

CORRELATION COEFFICIENT(CC)

-A measure of the correlation of the horizontal and vertical back scattered power within a radar sample volume.

VALUE	
0.96 to 1	*Small diversity in hydrometeors within the sample volume*
0.85 to 0.95	*Large diversity in hydrometeors*
Less than 0.85	*Non-hydrometeorological targets*

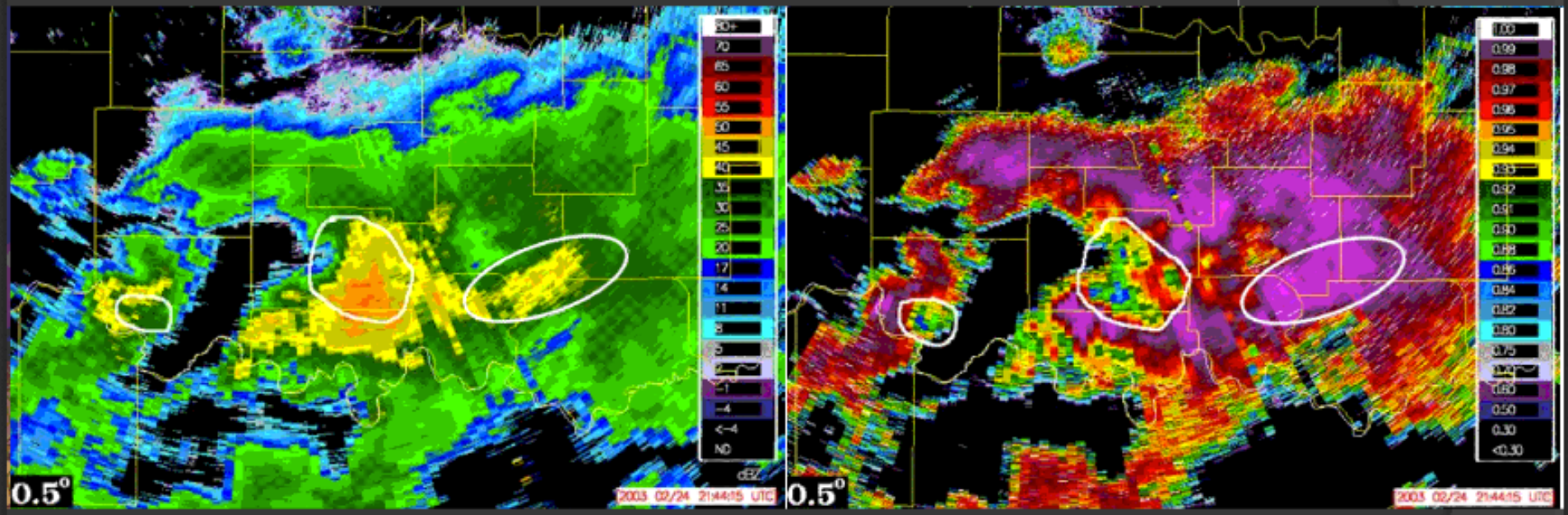

In this winter precipitation example, the area of high reflectivities on the right side of the left panel of traditional reflectivity is in an area of high correlation coefficient indicating hydrometeors of all the same size (likely all snow). The other two areas of higher reflectivity are characterized by lower values of CC indicated likely mixed precipitation.

ρ_{HV}–Correlation Coefficient. The correlation between the reflected horizontal and vertical power returns. ρ_{HV} is measured on a scale from 0 to 1 with values above 0.96-0.98 indicating hydrometeors with consistent size, shape, orientation and/or phase and values below 0.96 indicating a mixture of these within the sampled volume. Very large hail and non-precipitation echoes often indicate values of ρ_{HV} below 0.8. Large depressions in the correlation coefficient are also a good indicator for mixtures of liquid and frozen hydrometeors (e.g., snow and rain) in winter situations and in radar bright-bands.

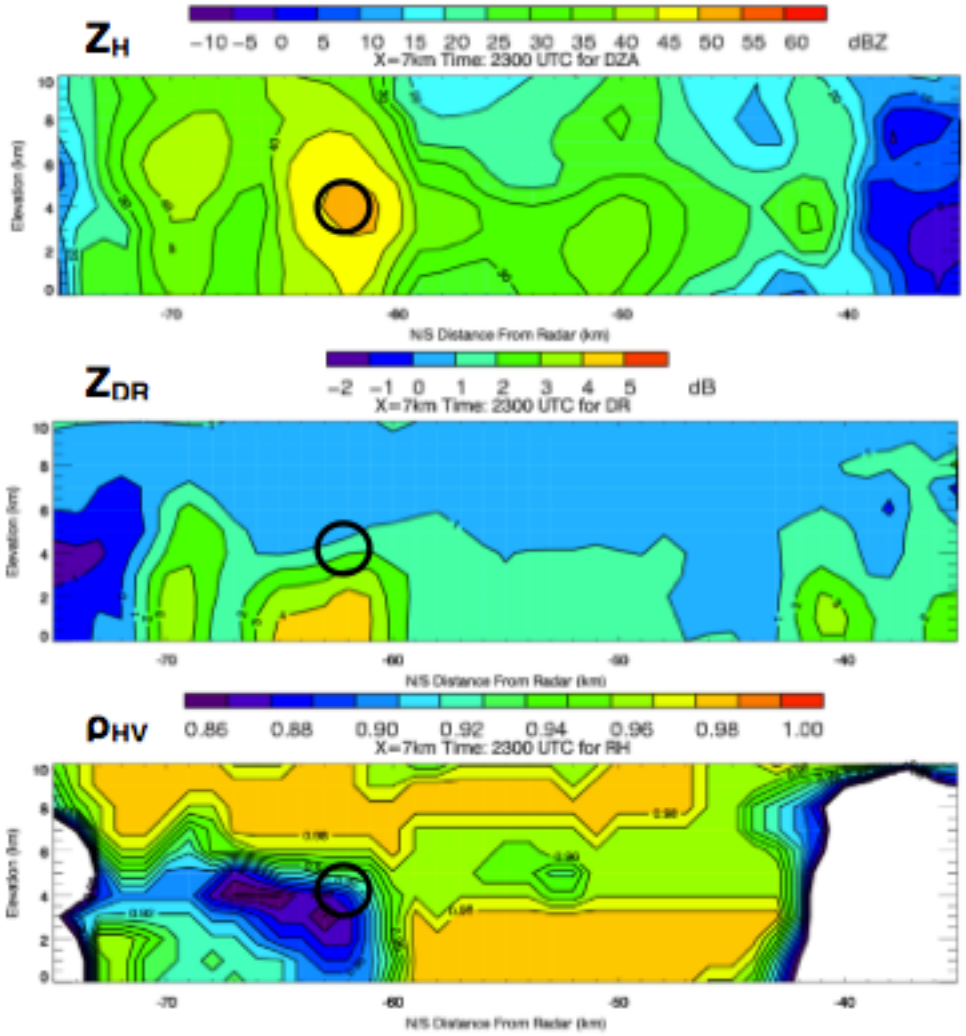

February 10, 2013 Tornado Hattiesburg, MS

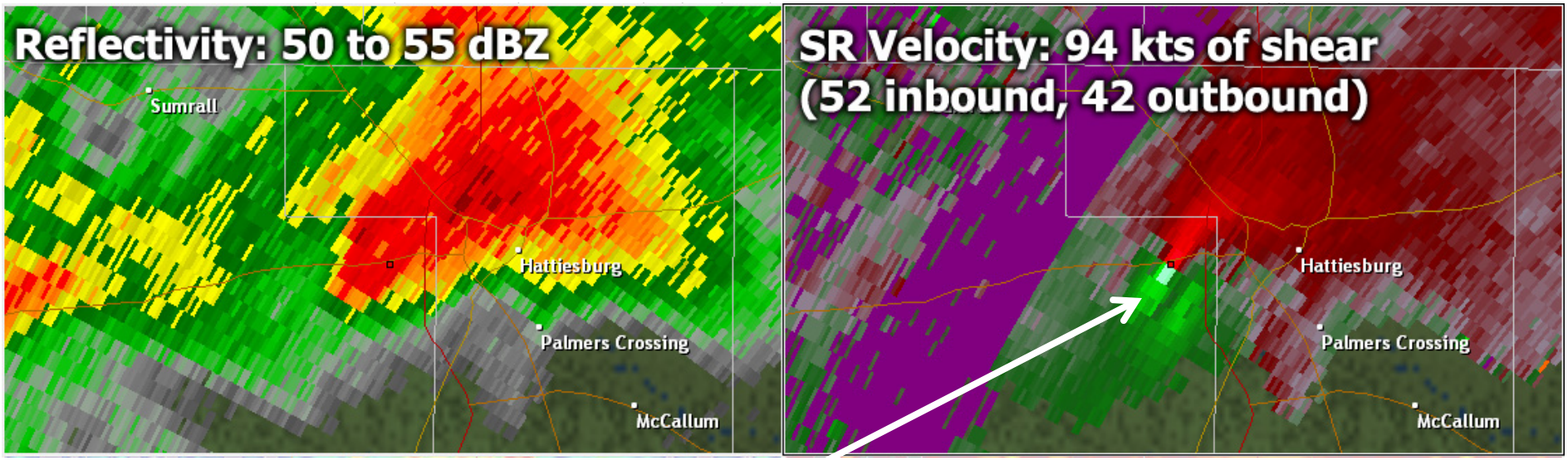

- Doppler radar reveals rotation in storm approaching Hattiesburg
- Without dual-pol, need spotters or “ground truth” to verify tornado

With Dual-pol: Confirmed

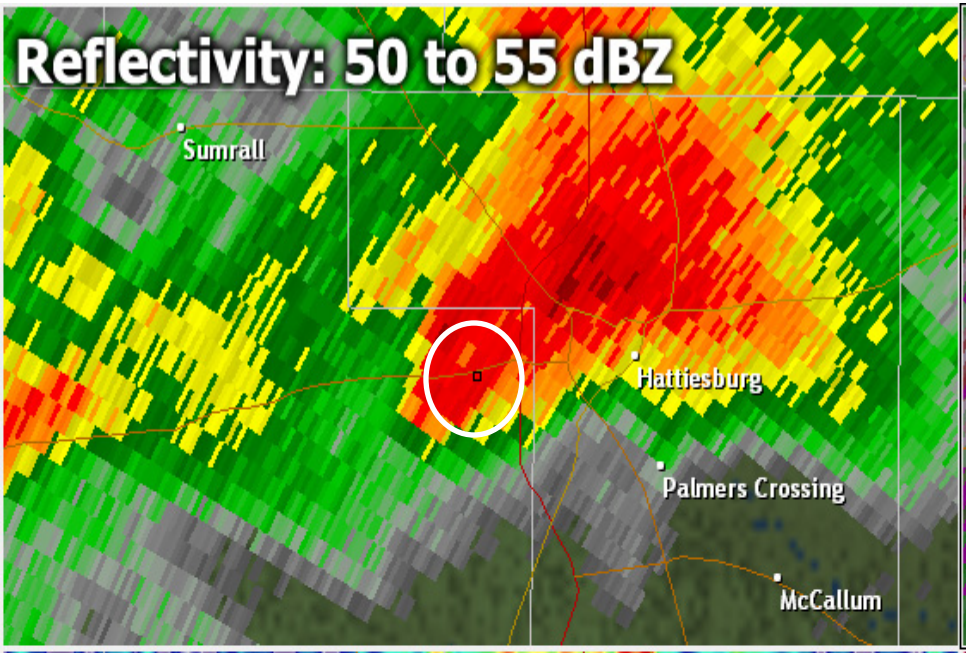

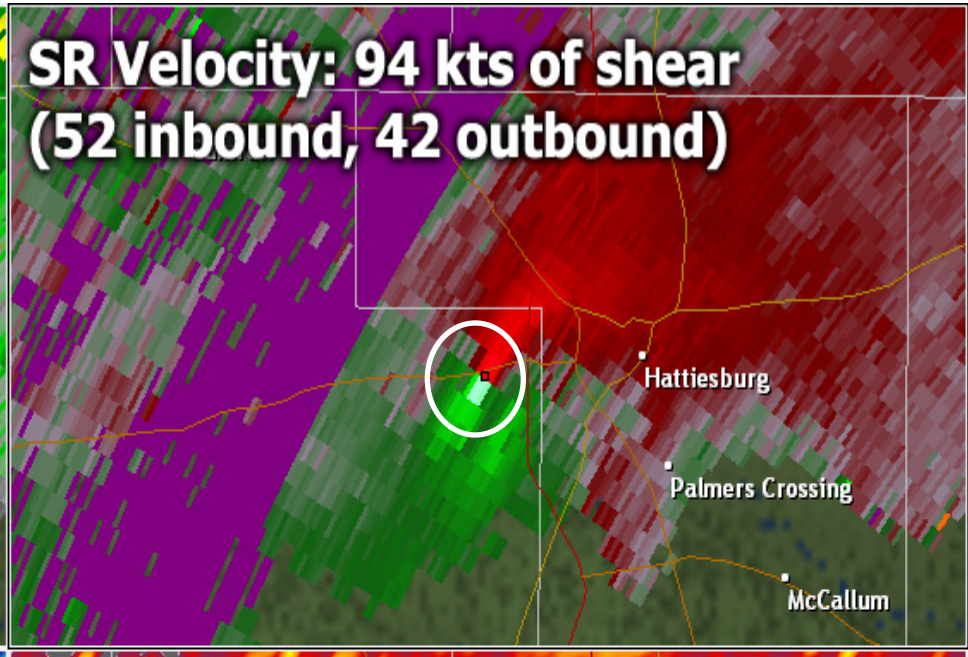

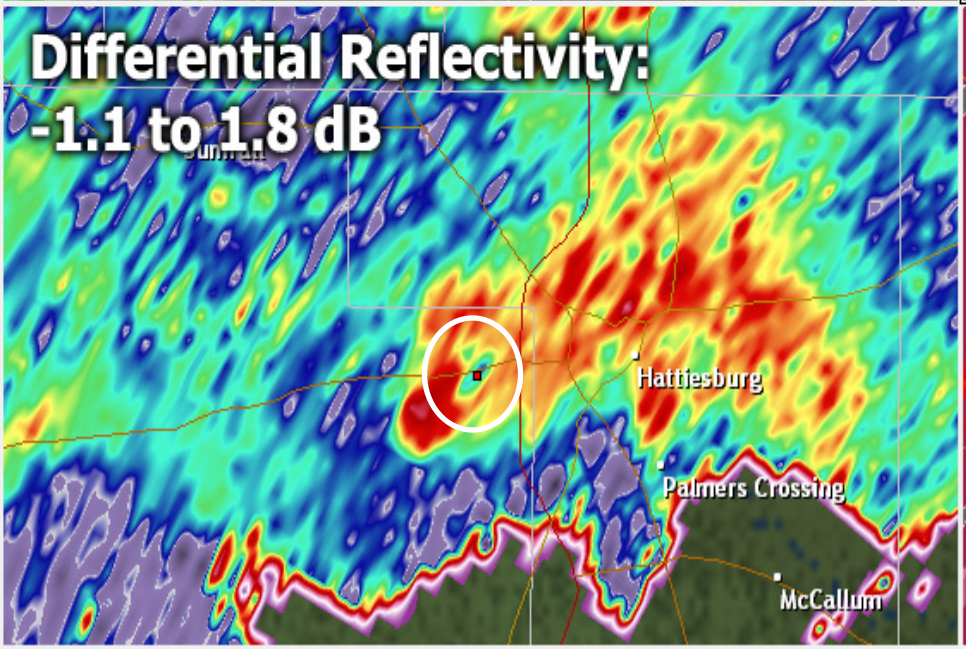

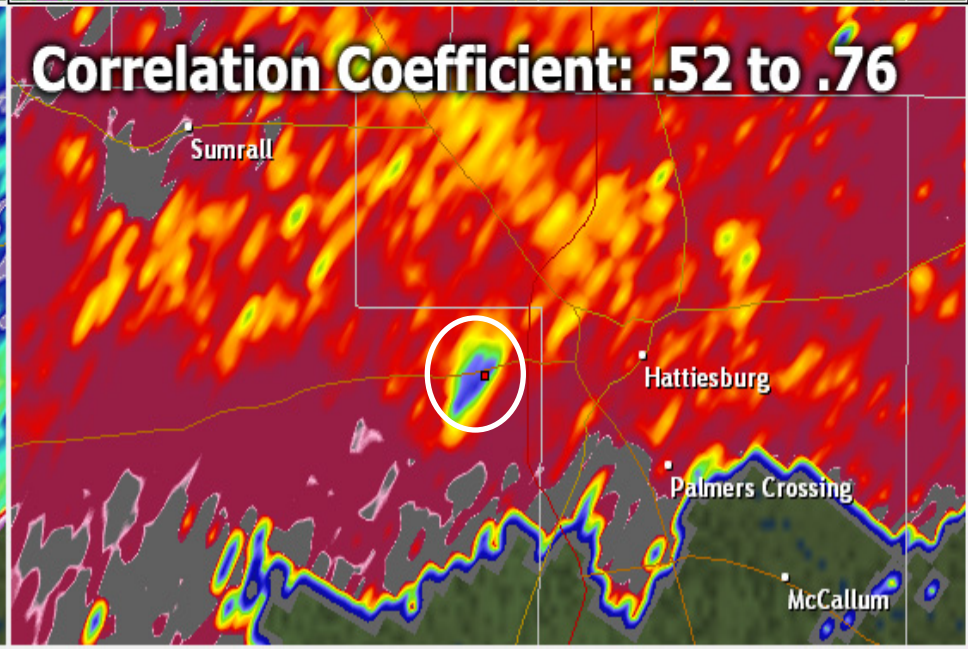

Differential Phase Shift Φ_{DP}

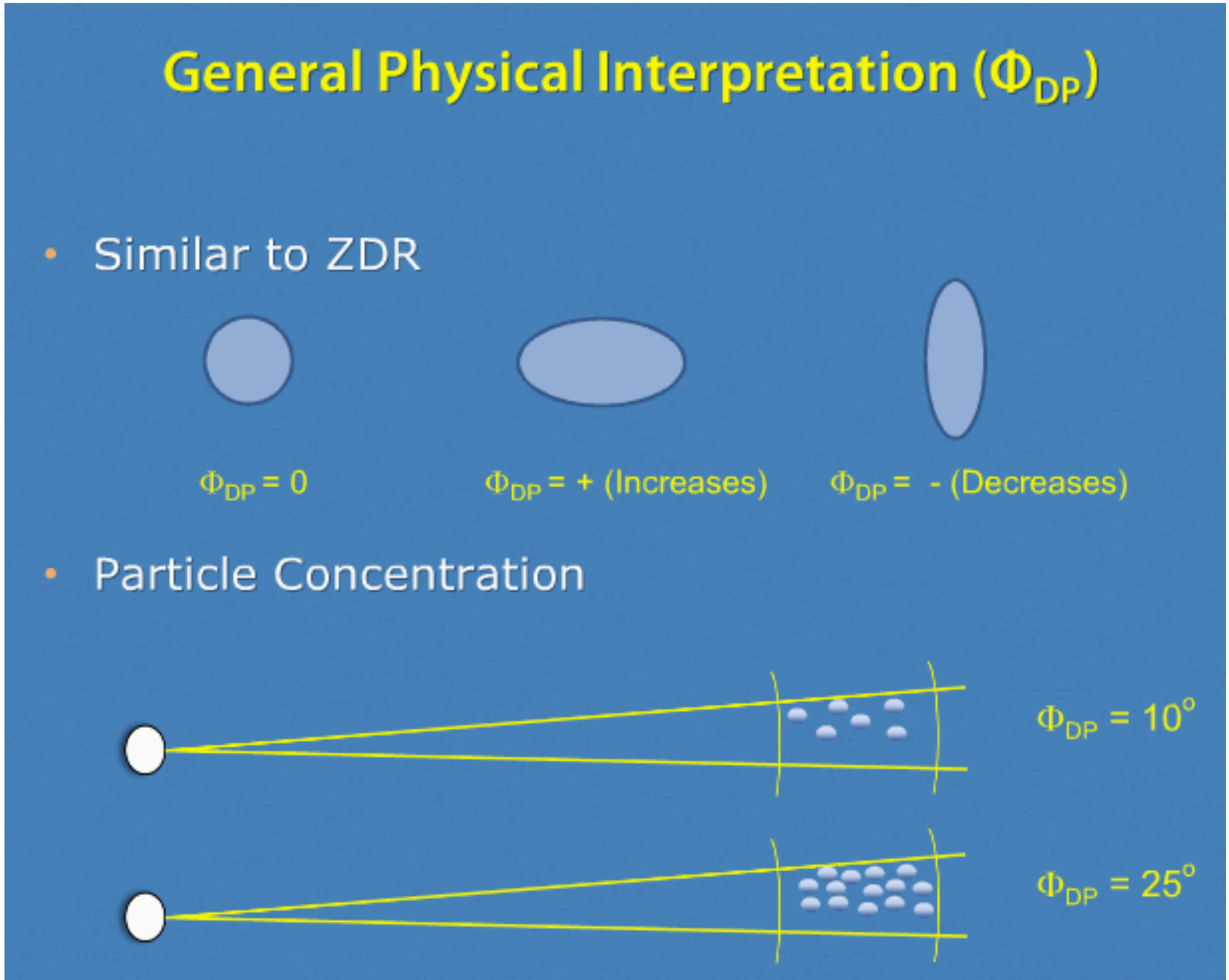

Specific Differential Phase (KDP)

Definition	Possible Range of Values	Units	Abbreviated Name
The range derivative of the differential phase shift between the horizontal and vertical pulse phases	-2 to 10	Degrees per Kilometer (deg/km)	KDP

$$KDP = \frac{\phi_{DP}(r_2) - \phi_{DP}(r_1)}{2(r_2 - r_1)}$$

- Definition
  - Range derivative of the differential phase shift along a radial
  - Units: deg/km
- General interpretation
  - High KDP in heavy rain
  - Hail/Snow/Ice Crystals = near 0 KDP
    - Exceptions:

      Preferential orientation of ice crystals

      Small, nearly melted hail
  - Non-meteorological echoes
    - Typically not shown because of CC < 0.90

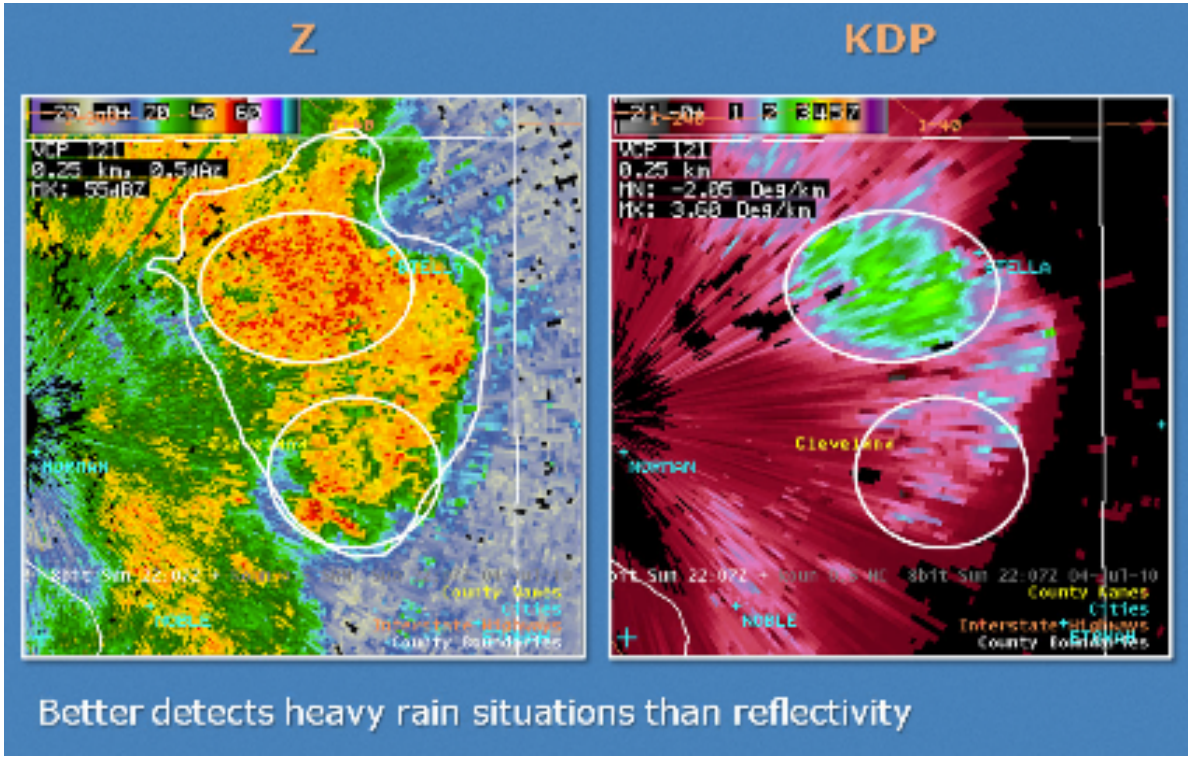

Instructor Notes: The primary advantage of KDP is its ability to detect heavy rain situations. Here is an example where we have a modest area (big white polygon) of greater than 40 dBZ echoes that is fairly uniform in intensity. Looking at KDP, we see higher KDP values to the north (top white oval), and lower KDP values to the south (bottom white oval) despite reflectivity values being almost identical. This tells us that there is heavy rain falling where the KDP values are higher and not as much rain where KDP is lower.